THE ASTRONOMICAL JOURNAL VOLUME 107, NUMBER 3 MARCH 1994

UBVRI PHOTOMETRY OF SN 1993J IN M81: THE FIRST 120 DAYS

MICHAEL W. RICHMOND
Department of Astrophysical Sciences, Princeton University, Princeton, New Jersey 08544
Electronic mail: richmond@astro.princeton.edu

RICHARD R. TREFFERS, ALEXEI V. FILIPPENKO,[1] AND YOUNG PAIK
Department of Astronomy University of California, Berkeley, California 94720
Electronic mail: treffers@bkyast.berkeley.edu, alex@bkyast.berkeley.edu, ypaik@goofy.berkeley.edu

BRUNO LEIBUNDGUT
European Southern Observatory, Karl-Schwarzschild-Strasse 2, D-8046 Garching bei Muenchen, Germany
Electronic mail: bleibund@eso.org

ERIC SCHULMAN AND CAROLINE V. COX
Department of Astronomy, University of Michigan, Ann Arbor, Michigan 48109-1090
Electronic mail: eric@astro.lsa.umich.edu, cvcox@astro.lsa.umich.edu

Received 1993 September 29; revised 1993 November 12

ABSTRACT

We present photometry of SN 1993J in M81 (NGC 3031) in the Johnson–Cousins *UBVRI* system, starting within three days of the probable time of explosion and ending 120 days later. The reddening along the line of sight to this supernova is uncertain—there is evidence for small [$E(B-V) \approx 0.08$ mag] and moderate [$E(B-V) \approx 0.32$ mag] values. For each value, we correct the observed fluxes for extinction and calculate the evolution of the sum of all optical flux, which contains roughly half of the supernova's total flux during the period of observation. We also fit the colors to a Planck function, and determine the temperature and total luminosity of the supernova for each value of reddening. A peculiar Type II supernova, SN 1993J gradually evolved spectroscopically to resemble a Type Ib in some respects. We compare its bolometric evolution with that of the prototypical Type Ib SN 1983N, and find the two to be similar.

1. INTRODUCTION

Soon after Francisco García reported his discovery of a supernova (SN) in M81 (NGC 3031) on 1993 March 28.9 UT (Ripero 1993), it became clear that SN 1993J would yield a treasure trove of information on supernovae. Its host galaxy is so nearby that the *Hubble Space Telescope* has been able to resolve Cepheids in its disk, yielding a relatively precise distance of 3.63 ± 0.34 Mpc (Freedman *et al.* 1993). Moreover, the high declination of M81 in the sky allowed some observers at mid-northern latitudes to follow the supernova continuously throughout the year. News of the discovery passed quickly through the electronic mail networks, and many observatories began monitoring the SN within forty-eight hours of the discovery.

The span of observations across the electromagnetic spectrum is enormous, approaching that of SN 1987A. In the brief list that follows, we note only the first few reports of detection in each portion of the spectrum, making no claims of completeness. CGRO may have detected the gamma-ray emission from SN 1993J, although the data are ambiguous at the current time and require further processing (NASA 1993). Both *ROSAT* (Zimmerman *et al.* 1993) and the newly launched ASCA (Tanaka 1993) satellites were able to detect x-rays from the supernova, and *HST* (Bowen *et al.* 1993) and *IUE* (Wamsteker *et al.* 1993) took spectra in the UV. Literally hundreds of observers followed the evolution of the optical emission. Several groups (Wheeler *et al.* 1993a,b; Calamai *et al.* 1993) obtained *JHK* photometry and infrared spectra. Phillips & Kulkarni (1993) made the first observations of any supernova at millimeter frequencies. Radio emission was reported starting about four days after discovery (Pooley & Green 1993; Weiler *et al.* 1993; Van Dyk *et al.* 1993) at 1.3 cm and progressively later at longer wavelengths. Jannuzi *et al.* (1993) and Trammell *et al.* (1993) measured significant polarization of the optical continuum. Finally, Aldering *et al.* (1994) have managed to collect a number of pre-explosion images which show an object at the location[2] of SN 1993J, making it only the second[3] supernova (after SN 1987A) for which we have some information on the

[1]Presidential Young Investigator.

[2]Morrison *et al.* (1993) report the following position from optical observations of SN 1993J with the Carlsberg Automatic Meridian Circle on La Palma: RA = $9^h55^m24^s.778$, Dec = $+69°01'13''.70$ (equinox J2000.0, FK5 reference frame), or, in B1950.0 coordinates, RA = $9^h51^m19^s.045$, Dec = $+69°15'26''.42$.

[3]Although pre-outburst images exist of SN 1961V, Goodrich *et al.* (1989) and Filippenko *et al.* (1994) argue that it should not be classified as a genuine supernova.

 0004-6256/94/107(3)/1022/19/$0.90

progenitor; it seems to have been a late G or early K supergiant (Aldering *et al.* 1994).

The first spectra showed a blue continuum with very weak lines of hydrogen (Filippenko *et al.* 1993; Garnavich & Ann 1993; Gomez & Lopez 1993) that quickly grew stronger, identifying SN 1993J as a Type II supernova. However, over the next month, the Balmer lines failed to become as strong as those in typical Type II SNe, and the Hα line gradually acquired a "double-peaked" appearance (due to superposed He I 6678). In early May, it became clear (Filippenko & Matheson 1993a; Filippenko *et al.* 1993; Swartz *et al.* 1993) that the spectrum was transforming itself into something which resembled that of a Type Ib supernova. Theorists have invented a designation for a class of such metamorphic objects, "Type IIb" (Woosley *et al.* 1987), and one other supernova, SN 1987K, has been observed to undergo such a change (Filippenko 1988). As the best-studied example of this new type, which may in turn shed light on the mysterious Type Ib, SN 1993J holds an especially important place in the supernova bestiary.

We discuss the optical light curve of SN 1993J, using *UBVRI* photometry from several sites and a small number of visual estimates at early times. In Sec. 2 we discuss the observations and data reduction, from which we create light curves in Sec. 3. We address the question of extinction along the line of sight in Sec. 4, which enters critically into the calculations of absolute magnitude (Sec. 5) and bolometric evolution (Sec. 6). In Sec. 7 we compare the behavior of SN 1993J in the optical with that of the Type Ib SN 1983N. We present our conclusions in Sec. 8. The Appendix contains details of the reduction of data from Leuschner Observatory. Our intent in this paper is to provide the astronomical community with accurate measurements of SN 1993J and an indication of their uncertainties, so that models may be constructed upon a firm foundation.

2. OBSERVATIONS

We include CCD photometry taken at several different sites in this study; most of the data were obtained at the Leuschner Observatory in California, but there are a number of points from Kitt Peak and from La Palma. We will discuss each site, its instrumentation, and characteristics of its data in turn. In addition, we examine some of the visual observations contributed by astronomers at early times.

2.1 Leuschner Observatory

Leuschner Observatory is located about fifteen kilometers east of Berkeley, California, at an elevation of 300 m above sea level. We used two telescopes to take images of the supernova: a 50 cm Cassegrain reflector and a 76 cm Ritchey–Chrétien reflector. A computer runs both telescopes, opening the domes at sunset, selecting objects to be observed, slewing from one field to the next, operating the shutter, and recording all the data (Richmond *et al.* 1993). Our earliest observations at Leuschner occurred on March 30.2 UT.

The 50 cm telescope has a set of *UBVRI* filters made to the specifications of Table 6 in Bessell (1990) and a Thomson 7895 CCD chip housed in a camera kept at -45 °C via closed-cycle liquid coolant. Each pixel on the chip subtends 0.″63 on the sky, giving a field of view of 5.′4 on a side. Although the 50 cm telescope has an autoguider, the guiding camera was out of service until June 3; as a result, all images before that time were short enough to avoid trails (typically 100 to 200 s). After June 3, we were able to increase exposure lengths to 1200 s, which greatly improved the signal-to-noise ratio.

The 76 cm telescope is equipped with *BVRI* filters as described in Table 1 of Schild (1983) and a Ford Aerospace CCD, 516×516 pixels in size, inside a camera similar to that on the 50 cm telescope. There is a "*U*" filter of unknown origin in the filter wheel, but we have determined that the effective passband it yields is so far from the standard Johnson *U* that one cannot reliably transform its measurements to the standard system (see Appendix). The scale is 0.″68 per pixel, and the field of view 5.′8 on a side. Since the 76 cm telescope lacks a guider, it cannot track accurately for more than a few minutes; our longest exposure times are 300 s.

The seeing at Leuschner is poor: The full width at half-maximum (FWHM) of stars in our 76 cm *I*-band images ranges from 2.″1 to greater than 5.″0, with a typical value of about 3.″0. Images in *R* and *V* usually have slightly larger values than in *I*, and those in *U* and *B* often have FWHM larger by 1.″0 or more, in addition to slight trails due to longer exposures. The 50 cm telescope performs even worse: its best images, in the *R* and *I* bands, have FWHM $\approx$3.″3, and about 0.″5 worse in *V*; the unguided *U* and *B* exposures are often trailed slightly.

We describe our reduction procedure in the Appendix. We measured the brightness of the supernova and stars A, B, C, and H (if possible), using apertures of fixed radius: 3.″4 for 76 cm images and 3.″2 for 50 cm images; we measured the sky value for each star as the median of values within an annulus with radii roughly 10″ and 13″. Aperture photometry may yield results that change with the seeing if the background is nonuniform. However, we found that only star A suffers significantly from this effect, because it alone lies in a region of M81 which varies appreciably across the sky annulus. Moreover, in the *U* and *B* bands, we detected so little emission from the disk of M81 that the background was essentially uniform around all the stars.

In order to convert our raw differential magnitudes to the standard Johnson–Cousins *UBVRI* system, we made corrections for first-order color terms, using coefficients determined from observations of the M67 "dipper" asterism and the field around PG 1633+009 (see Appendix). In addition, for the *B* band *only*, we correct for the differential extinction based on $(B-V)$ color. This effect is negligible for the *V*, *R*, and *I* bands; and, while certainly significant in the *U*, the relationship is sufficiently complex (Moffat & Vogt 1977) that we were unable to obtain enough calibration images to determine the coefficients accurately.

We then added a constant to the color-corrected differential magnitudes in order to give star *B* the values shown

TABLE 1. Johnson–Cousins magnitudes of stars close to SN 1993J.*

Star	U	B	V	R	I	source
A[1]	12.02 ±0.03	11.96 ±0.01	11.40 ±0.04	11.11 ±0.03	10.80 ±0.05	Kitt Peak
B[2]	12.32	12.40	11.90	11.60	11.30	Corwin 1993
	12.33 ±0.03	12.41 ±0.02	11.89 ±0.05	11.61 ±0.03	11.30 ±0.05	Kitt Peak
C[3]	15.08 ±0.08	15.10 ±0.07	14.58 ±0.11	14.21 ±0.12	13.83 ±0.05	Kitt Peak

[1] Also known as GSC 4383.928, and as star F on *The Astronomer* chart.
[2] Also known as GSC 4383.565.
[3] Also known as GSC 4383.340.

in Table 1, which were contributed by Corwin (1993), and are consistent with our own measurements (Sec. *2.2*). The resulting Leuschner light curves are presented in Tables 2 and 3. (These tables are presented in their complete form in the ApJ/AJ CD-ROM Series, Vol. 2, 1994.) We emphasize once again that the 76 cm telescope's *U*-band values do not transform well onto the standard color system, but may at least give a qualitative idea of the behavior of SN 1993J at near-UV wavelengths.

In order to determine the *internal* uncertainties in our photometry, apart from any systematic effects due to improper calibration, we examined the difference between the raw, instrumental magnitudes of the comparison stars A, B, and C. Stars A and B are both reasonably bright, but not as bright as SN 1993J at its peaks; moreover, star A sits within a brighter region of M81 than either star B or the SN (see Fig. 1). Neither star showed any evidence for variations above the level of 0.02 mag over the course of our observations. Therefore, the standard deviation of the difference $\Delta(AB) = \text{mag}(B) - \text{mag}(A)$ from its mean value ought to provide a conservative upper bound on the uncertainty in each individual measurement of the SN when it was bright. Star C, on the other hand, is about 3 mag fainter than star A, fainter than SN 1993J in all bandpasses and at all times during our period of observation. It has been claimed that C is a variable star (de Vaucouleurs

TABLE 2. Leuschner 76 cm observations of SN 1993J.*

UT Date	JD-2,440,000	U	B	V	R	I	comments
Mar 30.2	9076.7	...	...	10.65:	10.53:	10.67:	bad weather
Mar 31.2	9077.7	...	10.89	10.78	10.63	10.57	bad weather
Apr 02.2	9079.7	...	11.70	11.33	11.07	11.12	bad weather
Apr 03.2	9080.7	11.15	12.01	11.67	11.35	11.07	
Apr 06.2	9083.7	...	...	11.76	11.31	11.21	
Apr 07.22	9084.72	11.83	12.13	11.73	11.32	11.21	
Apr 07.30	9084.80	11.72	12.02	11.62	11.21	11.10	
Apr 08.24	9085.74	11.71	11.92	11.48	11.04	11.03	
Apr 08.32	9085.82	11.79	12.00	11.56	11.12	11.11	
Apr 10.23	9087.73	11.75	11.75	11.24	10.89	10.87	bad weather
Apr 10.40	9087.90	11.79	11.79	11.28	10.92	10.90	bad weather
Apr 11.21	9088.71	...	...	11.17	10.77	10.80	
Apr 13.2	9090.7	11.57	11.46	10.96	10.58	10.61	
Apr 13.3	9090.8	11.58	11.47	10.97	10.59	10.62	
Apr 14.2	9091.7	...	11.33	10.88	10.49	10.53	
Apr 14.3	9091.8	11.56	11.36	10.91	10.52	10.56	
Apr 16.2	9093.7	...	11.28	10.77	10.39	10.41	
Apr 16.3	9093.8	...	11.31	10.80	10.42	10.44	
Apr 17.2	9094.7	...	...	10.75	10.36	10.41	bad weather
Apr 18.3	9095.8	...	11.37	10.78	10.41	10.39	bad weather
Apr 20.3	9097.8	...	...	10.82	10.46	10.41	
Apr 22.2	9099.7	...	...	10.98	10.61	10.42	bad weather
Apr 23.2	9100.7	12.64	11.90	11.07	10.65	10.49	
Apr 23.3	9100.8	12.60	11.86	11.03	10.61	10.45	
Apr 25.2	9102.7	...	...	11.25:	10.72	10.58:	bad weather
Apr 27.3	9104.8	13.23	12.49	11.42	10.88	10.69	
Apr 28.3	9105.8	13.31	12.59	11.45	10.82	10.73	
Apr 29.2	9106.7	13.38	12.70	11.52	10.89	10.77	
Apr 30.3	9107.8	13.51	12.79	11.59	10.94	10.79	
May 01.2	9108.7	13.52	12.85	11.63	10.97	10.85	
May 02.2	9109.7	13.62	12.92	11.68	11.00	10.88	
May 03.2	9110.7	13.48	12.93	11.72	11.00	10.90	poor seeing
May 04.3	9111.8	13.53:	13.06	11.81	11.12	10.96	occasional clouds
May 05.2	9112.7	13.64	13.11	11.86	11.15	10.97	
May 07.2	9114.7	13.64	13.22	11.95	11.24	11.05	
May 09.3	9116.8	13.77	13.29	12.02	11.30	11.11	
May 10.3	9117.8	13.67	13.34	12.05	11.36	11.11	
May 11.2	9118.7	...	...	12.13:	11.42:	11.13:	bad weather
May 14.3	9121.8	13.63	13.43	12.17	11.49	11.24	
May 15.3	9122.8	13.78	13.43	12.18	11.50	11.23	
May 16.3	9123.8	13.63	13.50	12.23	11.57	11.28	
May 17.3	9124.8	13.61	13.50	12.23	11.56	11.28	
May 19.3	9126.8	...	...	12.31:	11.63:	11.34:	bad weather
May 21.3	9128.8	...	13.56:	12.33	11.65	11.38	bad weather
May 22.3	9129.8	13.89:	13.58	12.40	11.73	11.39	
May 23.3	9130.8	13.96	13.61	12.40	11.77	11.43	
May 28.2	9135.7	...	13.62	12.49:	11.87	11.53	bad weather
May 29.3	9136.8	...	...	12.48:	11.86:	11.56:	bad weather
Jun 03.3	9141.8	...	13.69:	12.58	11.91	11.63:	bad weather
Jun 08.2	9146.7	13.97	13.73	12.66	12.01	11.74	
Jun 09.2	9147.7	14.14	13.74	12.70	12.09	11.77	
Jun 11.3	9149.8	14.06:	13.77	12.76	12.16	11.79	bad weather
Jun 12.2	9150.7	14.02	13.76	12.75	12.13	11.81	
Jun 13.2	9151.7	13.98	13.76	12.76	12.14	11.84	
Jun 14.3	9152.8	13.98	13.78	12.78	12.19	11.85	
Jun 16.3	9154.8	13.98	13.80	12.82	12.22	11.90	
Jun 18.3	9156.8	13.99	13.79	12.82	12.19	11.94	
Jun 19.3	9157.8	13.89	13.82	12.84	12.22	11.97	
Jun 20.3	9158.8	13.86:	13.86	12.91	12.35	11.97	poor seeing
Jun 21.2	9159.7	...	...	12.89:	12.33:	11.92:	poor seeing, cloud
Jun 22.3	9160.8	13.77:	13.83	12.91	12.32	12.02	
Jun 23.2	9161.7	13.81	13.85	12.93	12.35:	12.01	
Jun 24.2	9162.7	13.98	13.87	12.97	12.38	12.05	light clouds?
Jun 25.2	9163.7	14.09	13.89	13.04	12.48	12.09	
Jun 26.2	9164.7	14.03	13.90	13.02	12.50	12.11	
Jun 27.2	9165.7	...	13.91	13.04	12.53	12.11	poor seeing
Jun 28.2	9166.7	14.13:	13.95	13.01	12.48	12.15	poor seeing
Jun 29.2	9167.7	14.08	13.94	13.09	12.57	12.15	
Jun 30.2	9168.7	14.15	13.95	13.08	12.55	12.18	
Jul 01.2	9169.7	14.11	13.97	13.12	12.57	12.21	
Jul 02.2	9170.7	14.28	13.95	13.10	12.57	12.21	
Jul 03.2	9171.7	...	13.87	13.13	12.58	12.21	poor seeing
Jul 04.2	9172.7	...	13.95	13.16	12.63	12.26	poor seeing
Jul 05.2	9173.7	14.04	13.97	13.17	12.61	12.25	
Jul 06.2	9174.7	...	14.01	13.19	12.66	12.32	poor seeing
Jul 09.2	9177.7	...	...	...	12.75	12.38	
Jul 11.2	9179.7	...	14.05	13.24	12.68	12.40	
Jul 12.2	9180.72	...	14.07:	13.25	12.74	12.44	clouds? poor seeing
Jul 13.2	9181.7	...	14.09	13.30	12.83	12.39:	
Jul 14.2	9182.7	...	14.15	13.40	12.89	12.47	poor seeing
Jul 15.2	9183.7	...	14.11	13.38	12.91	12.50	
Jul 16.2	9184.7	...	14.18	13.41	12.95	12.52	
Jul 17.2	9185.7	...	14.14	13.43	12.93	12.56	
Jul 18.2	9186.7	...	14.17	13.42	12.98	12.57	
Jul 19.2	9187.7	...	14.31+	...	13.00+	...	very poor seeing
Jul 20.2	9188.7	...	...	13.53	13.09	12.62	poor seeing

In the table above, ":" denotes an uncertain value, and "+" one which has been derived using color terms from the previous or following night.

*Table 2 is also presented in its complete form in the ApJ/AJ CD-ROM Series, Vol. 2, 1994.

TABLE 3. Leuschner 50 cm observations of SN 1993J.*

UT Date	JD[a]	U	B	V	R	I	notes[b]
Apr 03.2	9080.7	11.46	12.01	11.65	11.35	11.06	
Apr 06.2	9083.7	11.81	12.20	11.80	11.45	11.23	
Apr 07.2	9084.7	11.82	12.12	11.69	11.34	11.14	
Apr 08.2	9085.7	11.78	11.98	11.56	11.21	11.04	
Apr 10.2	9087.7	11.62:	11.80	11.31	10.99	10.86	CP
Apr 11.2	9088.7	11.50	11.64	11.21	10.89	10.76	
Apr 12.2	9089.7	11.40	11.57	11.09	10.79	10.69	
Apr 13.2	9090.7	11.30	11.47	11.00	10.70	10.61	
Apr 14.2	9091.7	11.31	11.43	10.95	10.66	10.57	
Apr 16.2	9093.7	11.16	11.35	10.84	10.54	10.44	
Apr 17.2	9094.7	11.22	11.31	10.79	10.46	10.43	CP
Apr 18.2	9095.7	11.34	11.35	10.76	10.44	10.35	CP
Apr 19.2	9096.7	11.34	11.38	10.75	10.45	10.38	
Apr 20.3	9097.7	11.49	11.48	10.83	10.49	10.39	
Apr 22.2	9099.7	11.58	11.71	10.95	10.57	10.47	CP
Apr 23.2	9100.7	12.12	11.87	11.03	10.61	10.45	
Apr 27.2	9104.7	13.36:	12.49	11.36	10.86	10.64	
Apr 27.3	9104.8	13.40	12.53	11.40	10.90	...	
Apr 28.3	9105.7	13.56	12.65	11.51	11.00	10.76	
Apr 29.2	9106.7	13.39	12.72	11.55	11.00	10.77	
Apr 29.3	9106.8	13.38	12.71	11.54	10.99	10.76	
May 01.2	9108.7	14.12	12.82	11.66	11.10	10.85	
May 02.2	9109.7	14.15	12.94	11.71	11.14	10.87	
May 03.2	9110.7	13.62	12.96	11.79	11.20	10.95	CP
May 08.2	9115.7	...	13.26	12.01	11.42	11.11	
May 09.3	9116.7	14.19	13.31	12.04	11.44	11.13	
May 14.3	9121.8	...	13.46	12.22	11.61	11.26	
May 15.3	9122.8	...	13.46	12.22	11.63	11.28	
May 16.3	9123.7	...	13.47	12.22	11.64	11.29	
May 19.3	9126.7	...	13.55	12.29	11.72	11.37	CP
May 21.3	9128.8	...	...	12.36	11.80	11.43	CP
May 22.3	9129.8	...	13.56	12.39	11.82	11.45	
May 23.3	9130.8	...	13.57	12.39	11.81	11.47	
Jun 03.3	9141.8	14.04	13.68	12.59	12.03	11.67	CP
Jun 09.2	9147.8	14.29	13.79	12.73	12.21	11.79	
Jun 27.2	9165.7	14.47	13.98	13.08	12.60	12.16	P
Jun 29.2	9167.7	14.30+	...	13.11+	...	12.21+	
Jun 30.2	9168.7	14.34	13.95+	...	12.65+	...	
Jul 01.2	9169.7	14.29+	...	13.11+	...	12.19+	
Jul 02.2	9170.7	14.26	13.96+	...	12.69+	...	
Jul 03.2	9171.7	...	...	13.13+	...	12.31+	P
Jul 04.2	9172.7	14.36	13.96+	...	12.72+	...	P
Jul 05.2	9173.7	14.35+	...	13.20+	...	12.30+	
Jul 06.2	9174.7	14.24	13.99+	...	12.80+	...	P
Jul 11.2	9179.7	14.49+	...	13.32+	...	12.47+	
Jul 12.2	9180.7	...	14.14	13.34	12.88	12.49	CP
Jul 13.2	9181.7	14.50+	...	...	...	...	

[a]Julian Date - 2,440,000.
[b]P = poor seeing; C = clouds.

In the table above, ":" denotes an uncertain value, and "+" one which has been derived using color terms from the previous or following night.

*Table 3 is also presented in its complete form in the ApJ/AJ CD-ROM Series, Vol. 2, 1994.

1993a), with an amplitude in V of about 0.3 mag. We find no evidence for any periodic variation. Looking at star H, which is similar in brightness to star C, we see that 76 cm observations yield similar deviations from the mean for the raw differences between pairs AC and AH. In any case, the standard deviation of $\Delta(AC) = \text{mag}(C) - \text{mag}(A)$ from its mean should certainly provide a conservative upper bound on the uncertainty in individual measurements of the SN at later times, when it was faint. We present the standard deviations of $\Delta(AB)$ and $\Delta(AC)$ in Table 4 for each telescope, and include $\Delta(AH)$ for the 76 cm telescope. Note that most of the magnitudes for SN 1993J we

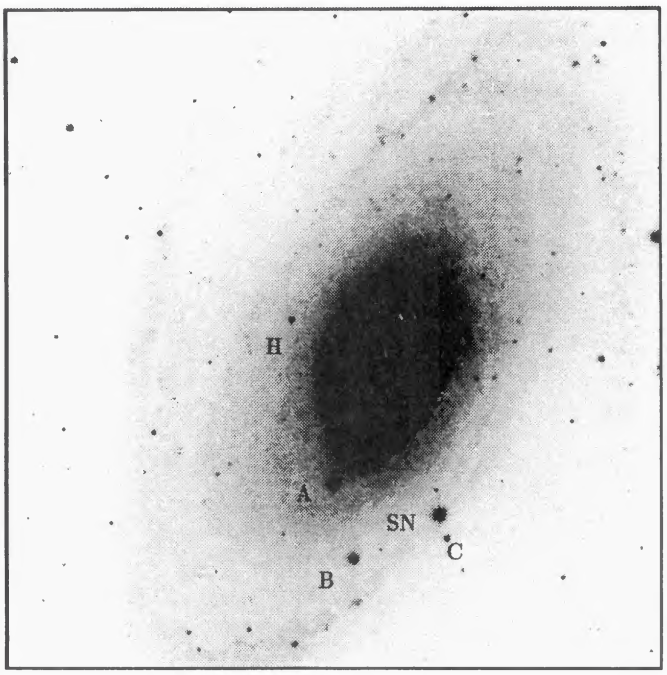

FIG. 1. Field of SN 1993J. North is at top, East to the left. The field of view is about 25′×25′. Courtesy of Brian Schmidt, Nelson Caldwell, Alexandra Milone, and the Center for Astrophysics.

list in Tables 2 and 3 are derived from an average of two or three frames, so that the internal uncertainties should be even smaller than indicated by the statistics of $\Delta(AB)$ and $\Delta(AC)$.

2.2 Kitt Peak

The Michigan–Dartmouth–MIT Observatory[4] is located on the southwest ridge of Kitt Peak, Arizona. We used the 1.3 m McGraw-Hill $f/7.5$ Cassegrain reflector during April 14–26 UT to observe SN 1993J.

The data were taken with a Thomson-CSF TH7861 CCD with a scale of 0.″474 pixel^{-1}, yielding a field of view 3.′0×4.′5. We used MDM filter set #1, described in Table 5, which differs from the Johnson–Cousins system most strongly in the I band; the I filter has no long-wavelength cutoff, and is limited only by the response of the CCD and atmospheric transmission.

The seeing varied from 0.″7 to 2.″5 (FWHM), with a typical seeing of about 1″. Our exposure times varied from 300 to 1200 s in U, 100 to 300 s in B, 12 to 40 s in V, 5 to 20 s in R, and 5 to 30 s in I. The typical exposure times were 300 s in U, 100 s in B, 20 s in V, 10 s in R, and 12 s in I. The night of Apr 23 UT was very cloudy and the exposure times were increased to 1200 s in B and 600 s in V, R, and I in order to obtain enough photons. It was not possible to obtain an accurate U measurement on this night.

The following steps were followed for each night of observations: During the early afternoon, we took a series of

[4]MDM Observatory is operated by the University of Michigan, Dartmouth College, and the Massachusetts Institute of Technology.

TABLE 4. Internal accuracy of Leuschner magnitudes.[a]

stars	U	B	V	R	I
			76-cm telescope		
AB	0.075	0.019	0.020	0.031	0.015
AC	0.165	0.069	0.054	0.032	0.064
AH	0.198	0.105	0.060	0.071	0.047
			50-cm telescope		
AB	0.109	0.026	0.016	0.016	0.038
AC	0.488	0.138	0.088	0.044	0.051

[a] Standard deviation from the mean values of raw differences between the indicated pairs of stars.

five exposures through each of the *U*, *B*, and *V* filters of an illuminated white screen on the inside of the dome. At sunset, we took a series of five exposures of the twilight sky through the *R* and *I* filters, moving the telescope 30″ between each 5 s exposure in case there were any bright stars in the field. During the night, we observed the supernova and between 10 and 30 Landolt (1992) standards in *UBVRI*. The bias level for each frame was taken from the overscan region and subtracted from every pixel in the image, the flatfield frames were medianed and normalized, and each object frame was divided by a normalized flatfield image. Since the Thomson dark current is negligible, no dark count corrections were made.

As with the Leuschner data, we measured differential magnitudes via an aperture of fixed size, radius 4.″0, around each star, using the mode of values within an annulus with radii 10″ and 20″ to determine the sky background. Pixel values differing from the mean by more than 3σ were not used in the sky value determination. We transformed the raw differential magnitudes onto the standard system using observations of Landolt (1992) standards, making individual solutions for each night of observations (except for the nights of Apr 16 and 23 UT, which were so cloudy that we could make differential measurements only). The solutions include first-order extinction and first-order color terms.

In order to check the quality of the transformation onto the standard color system, we have solved for the magnitudes of stars A, B, and C from the individual photometric solutions of the eight best nights. The means and standard deviations are listed in Table 1. Note that the difference between the mean values from Kitt Peak observations of star B and the Corwin values is less than 0.02 mag in all filters.

For consistency with the Leuschner observations, we have adopted the Corwin values and adjusted the Kitt Peak measurements so that star B is forced to agree with them; in essence, we perform differential photometry between the SN and star B, making corrections for first-order color terms. These magnitudes for SN 1993J are given in Table 6 (this table is presented in its complete form in the ApJ/AJ CD-ROM Series, Vol. 2, 1994), and will be used throughout this paper.

TABLE 5. Schombert filters at the MDM Observatory.

Filter	Glass
U	Schott UG-1, WG-280, Hoya CM-500
B	Schott BG-12, BG-39, GG-385
V	Schott GG-495, BG-18
R	Schott OG-570, KG-3
I	Schott RG-715

TABLE 6. Kitt Peak observations of SN 1993J.*

UT Date	JD-2,440,000	U	B	V	R	I	comments
Apr 14.17	9091.67	11.35	11.45	10.98	10.66	10.55	
Apr 15.15	9092.65	11.34	11.40	10.91	10.60	10.48	
Apr 16.19	9093.69	11.34	11.39	10.89	10.53	10.43	thin clouds
Apr 17.19	9094.69	11.37	11.39	10.84	...	10.39	clouds
Apr 18.15	9095.65	11.40	11.41	10.84	10.48	10.37	thin clouds
Apr 18.24	9095.74	11.42	11.40	10.81	10.49	10.37	thin clouds
Apr 19.15	9096.65	11.48	11.45	10.86	10.49	10.37	
Apr 20.15	9097.65	11.62	11.53	10.86	10.50	10.38	
Apr 21.28	9098.78	11.78	11.67	10.91	10.55	10.41	
Apr 22.15	9099.65	11.98	11.79	11.00	10.60	10.41	
Apr 23.25	9100.75	...	11.96	11.12	10.66	10.46	clouds
Apr 24.15	9101.65	12.52	12.14	11.18	10.72	10.51	
Apr 25.17	9102.67	12.75	12.32	11.31	10.79	10.58	
Apr 26.25	9103.75	13.02	12.44	11.39	10.86	10.65	

*Table 6 is also presented in its complete form in the ApJ/AJ CD-ROM Series, Vol. 2, 1994.

2.3 La Palma

We include photometry from the La Palma[5] data archives, retrieved in reduced form via FTP (Martin & Lewis 1993). Most of the measurements are from CCD images made by the 1 m Jacobus Kapteyn Telescope, with a few additional values from CCD images taken at the prime focus at the 2.5 m Isaac Newton Telescope. Details of the observations and reduction techniques can be found in Lewis *et al.* (1993). The La Palma data are shown in Table 7. (This table is presented in its complete form in the ApJ/AJ CD-ROM Series, Vol. 2, 1994.)

2.4 Visual Estimates

The earliest part of the history of SN 1993J, the initial rise to the first peak, is not covered by any photoelectric or CCD observations. We therefore present a selection of visual estimates, reported from a variety of institutions and distributed widely by electronic networks. In order to reduce the volume of such estimates, as well as the large scatter among them, we have binned the estimates within intervals of 0.5 days and taken the median value within each bin. There were several different charts of comparison star magnitudes used by the observers, which might introduce systematic offsets. We have checked to see if such offsets appear when those values obtained by comparison with one chart are compared with those for another. We find that, while there are hints of small differences ($\leqslant$0.2 mag), there is no unequivocal effect, at least among the reference charts most commonly used. Moreover, the deviation of median values from a smooth curve is minimized

[5]The Isaac Newton Group of telescopes is operated on the island of La Palma by the Royal Greenwich Observatory in the Spanish Observatorio del Roque de los Muchachos of the Instituto de Astrofisica de Canarias.

TABLE 7. La Palma[a] observations of SN 1993J.*

UT Date	JD[b]	U	B	V	R	I	notes[c]
Mar 30.89	9077.39	9.95	10.77	10.70	10.60	10.51	
Mar 31.06	9077.56	10.02	10.85	10.76	10.64	10.55	
Mar 31.98	9078.48	10.55	11.21	11.02	10.83	10.69	
Apr 01.90	9079.40	11.05	11.57	11.30	11.05	10.84	
Apr 02.99	9080.49	11.48	11.91	11.62	11.32	11.03	
Apr 03.16	9080.66	...	11.93	11.64	11.26	10.97	
Apr 03.90	9081.40	11.76	12.14	11.79	11.41	11.19	
Apr 04.09	9081.59	11.80	12.19	11.81	11.47	11.23	
Apr 04.95	9082.45	11.85	12.28	11.90	11.52	11.27	
Apr 05.08	9082.58	11.88	12.29	11.92	11.51	11.28	
Apr 05.91	9083.41	11.93	12.27	11.86	11.47	11.23	
Apr 05.97	9083.47	11.94	12.27	11.88	11.44	11.26	
Apr 06.10	9083.60	11.93	12.26	11.86	11.45	11.24	
Apr 06.99	9084.49	11.95	12.21	11.80	11.38	11.17	
Apr 08.02	9085.52	11.90	12.07	11.64	11.24	11.09	I
Apr 08.10	9085.60	11.89	12.06	11.63	11.25	11.10	
Apr 08.98	9086.48	11.78	11.95	11.50	11.11	10.96	
Apr 10.07	9087.57	11.70	11.82	11.39	11.04	10.91	
Apr 10.16	9087.66	11.69	11.82	11.36	11.02	10.94	
Apr 10.89	9088.39	11.63	11.73	11.28	10.83	10.78	
Apr 10.93	9088.43	11.63	11.72	11.29	10.83	10.74	
Apr 11.01	9088.51	11.65	11.73	11.28	10.86	10.82	
Apr 11.06	9088.56	11.66	11.74	11.32	10.85	10.81	
Apr 11.93	9089.43	...	11.64	11.17	...	...	
Apr 12.87	9090.37	...	11.51	11.10	...	...	
Apr 13.00	9090.50	...	11.53	11.08	...	...	
Apr 13.88	9091.38	...	11.48	11.01	...	...	
Apr 14.04	9091.54	...	11.46	11.00	...	...	
Apr 14.88	9092.38	...	11.42	10.94	...	...	
Apr 14.98	9092.48	...	11.40	10.93	...	...	
Apr 15.88	9093.38	...	11.38	10.89	...	...	
Apr 16.05	9093.55	...	11.39	10.90	...	...	
Apr 16.89	9094.39	...	11.37	10.87	...	...	
Apr 17.00	9094.50	...	11.38	10.85	...	...	
Apr 17.93	9095.43	...	11.40	10.90	...	...	
Apr 21.96	9099.46	...	11.73	10.99	10.54	10.40	
Apr 23.91	9101.41	...	12.04	11.16	10.66	10.49	
Apr 24.89	9102.39	...	12.22	11.24	10.82	10.60	
Apr 25.91	9103.41	12.94	12.36	11.35	10.77	10.62	
Apr 27.91	9105.41	13.33	12.64	11.51	10.88	10.73	
Apr 28.87	9106.37	13.45	12.78	11.63	10.94	10.81	
Apr 29.90	9107.40	13.63	12.82	11.68	10.98	10.79	
May 30.88	9108.38	13.70	12.94	11.72	11.03	10.86	
May 05.89	9113.39	14.10	13.26	12.01	11.28	11.05	
May 14.90	9122.40	14.43	13.51	12.26	11.56	11.28	
May 15.90	9123.40	14.37	13.54	12.32	11.60	11.30	
May 16.88	9124.38	...	13.58	12.32	...	...	
May 22.88	9130.38	14.41	13.63	12.45	11.76	11.46	
May 24.91	9132.41	14.44	13.71	12.48	11.81	11.49	P
May 25.88	9133.38	14.43	13.70	12.49	11.83	11.52	

[a]Data from the 1-m Jacobus Kapteyn Telescope unless marked I.
[b]Julian Day - 2,440,000.
[c]P = poor conditions; I = Isaac Newton Telescope.

*Table 7 is also presented in its complete form in the ApJ/AJ CD-ROM Series, Vol. 2, 1994.

when we include all estimates in our calculations. Therefore, we have included all the early estimates in this paper.

We note that there is an obvious color-dependent difference between the visual estimates and simultaneous CCD measurements in the V band. When the SN is blue, soon after discovery, visual estimates are brighter than V measurements; when the SN is red, at later times, the visual estimates are fainter. The dependence of this difference on the $(B-V)$ color of the SN is shown in Fig. 2, together with data for the Type Ia SN 1991T [visual estimates from Mattei (1993), CCD V and $(B-V)$ values from Phillips *et al.* (1992)]. Both SNe follow a similar pattern, despite

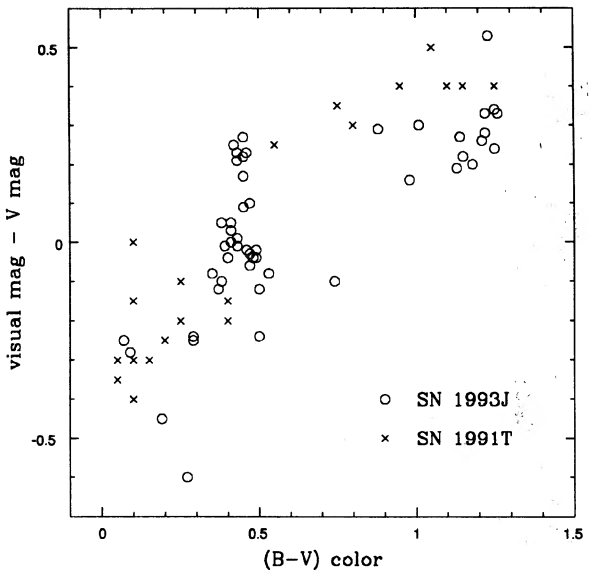

FIG. 2. Comparison of visual and V-band observations of SNe 1993J and 1991T.

the difference in their types. We find a relationship, using a linear fit to data from both SNe, of

$$m^*_{\rm vis} = \text{visual} - 0.266 + 0.53(B-V),$$

with a scatter of about 0.15 mag and a formal uncertainty of 0.03 in the coefficient of the $(B-V)$ term. We extrapolate backwards in time to find the color of the SN, using a linear relationship based on the first four measurements from La Palma with a slope of about 0.1 mag per day (very early observations of SN 1987A (Shelton 1993) show a roughly linear change in $(B-V)$ for the first ten days or so after core collapse). In Table 8 (this table is presented in its complete form in the ApJ/AJ CD-ROM Series, Vol. 2, 1994), we list "raw" visual magnitudes, formed by taking the median of all reported measurements within 0.5 day bins, together with the "corrected" $m^*_{\rm vis}$ values calculated from the above equation and extrapolated $(B-V)$ color.

TABLE 8. Early visual observations of SN 1993J.*

UT Date[a]	JD-2,440,000[a]	raw[b]	corrected[c]
Mar 29.14	9075.64	11.8	12.1
Mar 29.64	9076.14	11.2	11.5
Mar 30.14	9076.64	11.0	11.3
Mar 30.64	9077.14	10.4	10.6
Mar 31.14	9077.64	10.5	10.7
Mar 31.64	9078.14	10.5	10.7
Apr 01.14	9078.64	10.6	10.8
Apr 01.64	9079.14	10.6	10.7
Apr 02.14	9079.64	10.8	10.9
Apr 02.64	9080.14	11.3	11.4
Apr 03.14	9080.64	11.4	11.5

[a]The given date is that of the middle of the bin.
[b]Median of all observations within 0.5-day bin.
[c]See text §2.4 for details.

*Table 8 is also presented in its complete form in the ApJ/AJ CD-ROM Series, Vol. 2, 1994.

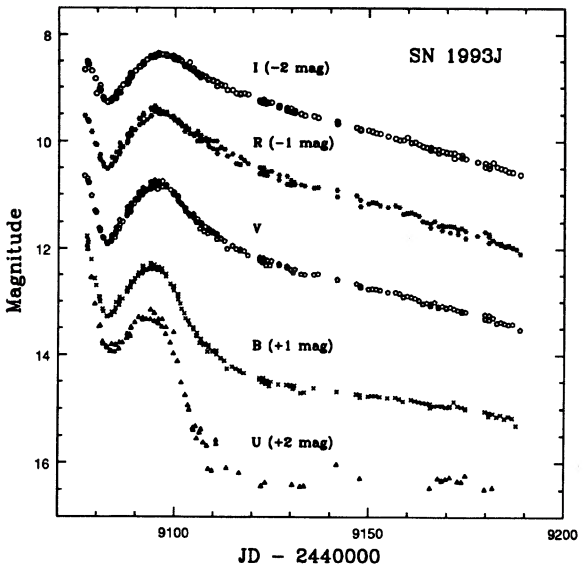

FIG. 3. *UBVRI* light curves of SN 1993J. The Leuschner 76 cm *U*-band data are omitted, since they are poorly calibrated.

3. LIGHT CURVES

In Figs. 3 and 4(a)–4(e) we present the light curves of SN 1993J in the Johnson–Cousins *UBVRI* passbands during the period 1993 March 29, to 1993 July 20, including data from Leuschner, Kitt Peak, and La Palma; in Figs. 5(a)–5(d) we show the evolution of the color curves. The *B*, *V*, and *I* curves show good agreement among data points from different instruments, but the *R* and *U* curves do not. The *U*-band data from the Leuschner 76 cm telescope, as mentioned above, are known not to be calibrated well; at late times, they are clearly offset by over a magnitude from values of other telescopes. However, we include them in Fig. 4(a) in order to give an impression of the behavior of the SN in *U*: a very slight decline, much less steep than that in other bands. Figure 4(d) reveals smaller offsets between the *R*-band datasets, which are shown more clearly in the $(V-R)$ and $(R-I)$ color curves [Figs. 5(c) and 5(d)]. The Cousins *R* bandpass has a very long tail toward the red, an imitation of the gradual decrease in sensitivity of photodiodes. If two instruments have slightly different tails, and if strong emission or absorption lines happen to fall in this tail, appreciable differences in photometry can result. The large difference between CTIO and SAAO *I*-band photometry of SN 1987A (Hamuy *et al.* 1990) is a more extreme example of the problem.

The outstanding feature of these light curves is the initial, short-lived peak, seen clearly in the combined visual-plus-*V* graph. This very early phase of supernova evolution, the result of the explosion's shockwave heating the photosphere to very high temperature, has very seldom been observed due to its brief duration. The best example of the phenomenon is SN 1987A, for which photometry was obtained within one day of core collapse (Hamuy *et al.* 1988; Shelton 1993). Unfortunately, we do not know

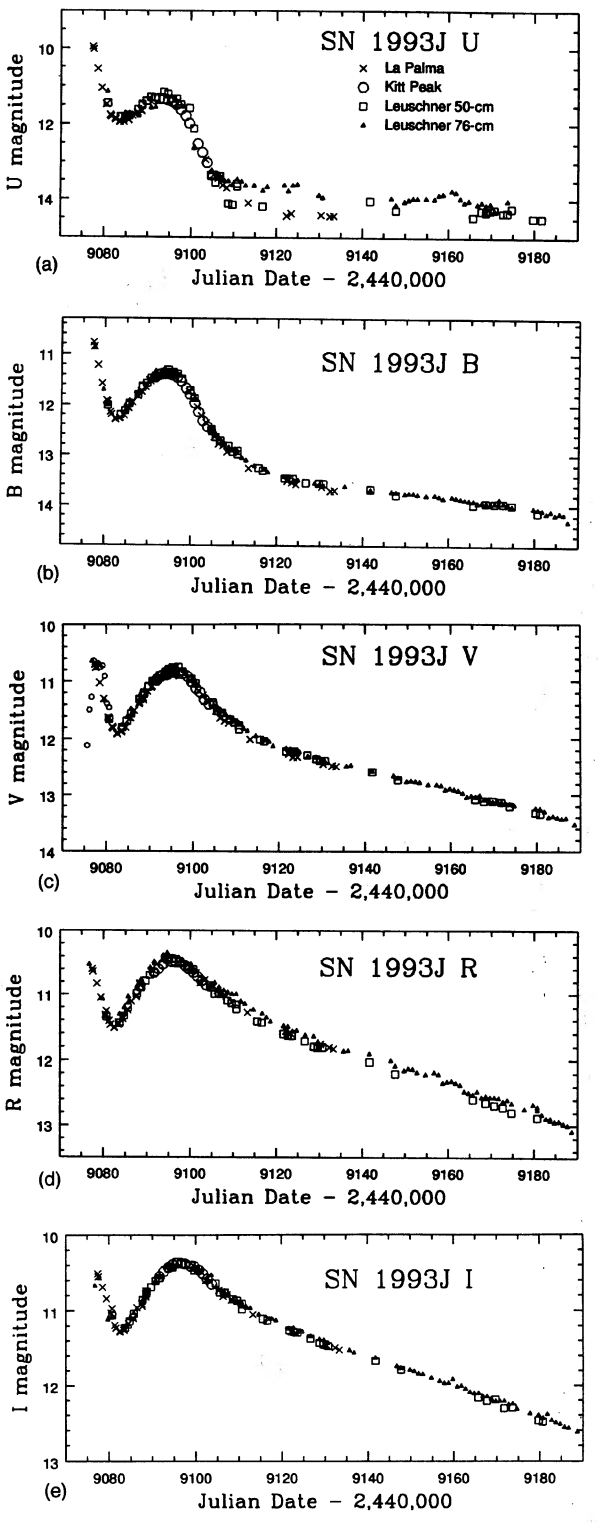

FIG. 4. (a) *U*-band light curve of SN 1993J. Note that the Leuschner 76 cm data points are poorly calibrated, and are included only to give a qualitative feel for the light curve's behavior. (b) *B*-band light curve of SN 1993J. Symbols as in (a). (c) *V*-band light curve of SN 1993J. Symbols as in (a). The small open circles are "corrected" visual values (see Sec. *2.4*). (d) *R*-band light curve of SN 1993J. Symbols as in (a). The slight difference between the Leuschner 76 and 50 cm points is a systematic offset due to difficulties in calibration. (e) *I*-band light curve of SN 1993J. Symbols as in (a).

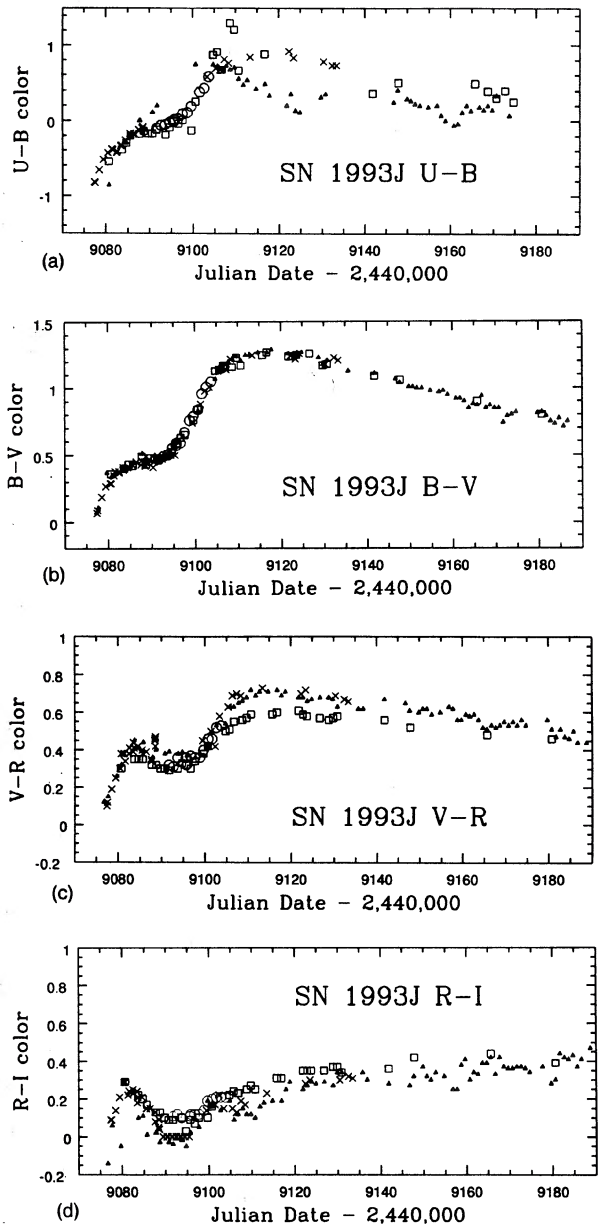

FIG. 5. (a) $U-B$ color curve of SN 1993J. Symbols as in Fig. 4(a). (b) $B-V$ color curve of SN 1993J. Symbols as in Fig. 4(a). (c) $V-R$ color curve of SN 1993J. Symbols as in Fig. 4(a). (d) $R-I$ color curve of SN 1993J. Symbols as in Fig. 4(a).

exactly when the core of SN 1993J's progenitor imploded (nor would we expect to detect the neutrino pulse; M81 is roughly seventy times more distant than the LMC, hence the flux of neutrinos from SN 1993J would be roughly 1/5000 that from SN 1987A—for which about twenty neutrinos were detected). However, based on the last nondetection, ($m \geqslant 16$) from a photograph taken on March 27.9 UT (Merlin 1993), the earliest detection, ($m_v \approx 13.5$) in an unfiltered CCD image taken on March 28.3 UT (Neely 1993a,b), and the rise of ~ 2 mag in the next twenty-four hours, we estimate that core collapse occurred during the period March 27.7–28.1. The earliest observations, therefore, probably occur within 15 h of the implosion, and the first of our own CCD observations within about sixty hours.

TABLE 9. Late-time slopes of light curves, in mag/day.

SN	U	B	V	R	I	source
1993J	~0.006	0.0103	0.0189	0.0220	0.0201	Leuschner 50-cm
1993J	~0.004	0.0098	0.0185	0.0219	0.0200	Leuschner 76-cm
1987A	~0.0	0.007	0.010	0.008	0.009	Hamuy & Suntzeff 1990

After its initial peak, SN 1993J dimmed by a little more than 1 mag in V. The photosphere was at this time cooling rapidly, as the evolution of the $(U-B)$ and $(B-V)$ color curves shows [Figs. 5(a) and 5(b)]. However, after reaching a minimum on April 6, the SN began to brighten again, attaining a second maximum around April 18. Note that, while the minimum occurs simultaneously in all colors, the second peak occurs earlier in the blue than in the red (see Table 12). After this peak, the SN's optical flux decreased sharply, especially in U and B. The very short duration of the second peak is an indication of the small mass of the SN's envelope (Nomoto *et al.* 1993; Woosley *et al.* 1993; Podsiadlowski *et al.* 1993; Ray *et al.* 1993; Wheeler *et al.* 1993b): high-energy photons from the inner regions of the ejecta can escape relatively easily instead of being absorbed and reradiated as optical photons, leading to increased levels of x-ray and gamma-ray emission and a diminished optical flux.

At late times, after May 10 or so, the light curve exhibits a linear decline in B, V, R, and I magnitudes, with slopes given in Table 9. Note that, while the V, R, and I curves have similar slopes, around 0.02 mag per day, the B curve has a much smaller slope, about half that size. The difference is far larger than the uncertainty in any of the slope values. The U-band light curve, fragmentary and noisy as it is, exhibits a decline even slower than that of B. This pattern is similar to that seen in SN 1987A, which maintained a relatively constant brightness in U for over a year, from the end of hydrogen recombination around day 125 until the beginning of dust formation around day 500 (Hamuy & Suntzeff 1990). Over this period, SN 1987A also faded much more rapidly at long wavelegths than at short ones—see Fig. 7 of Hamuy & Suntzeff (1990); these authors attribute the differences in rate of decline to differences in the opacity of the ejecta as a function of wavelength. Note that, while the trend of faster decline at longer wavelengths is shared by SNe 1993J and 1987A, the rates themselves are quite different: as Table 9 shows, the rate of decline, in magnitude per day, is about twice as large in SN 1993J as in SN 1987A. In fact, the decline of SN 1993J in VRI is roughly twice as fast as that produced by the radioactive decay of ^{56}Co (0.0098 mag per day).

4. REDDENING

The extinction along the line of sight to SN 1993J is crucial to any analysis of the photometry, and we therefore devote to it a large section of this paper. Unfortunately, at the time of writing, the amount of extinction is not known very well. There are a number of indicators, but they do

TABLE 10. Interstellar extinction conversion factors.

band	λ_{eff}^{a}	$R = A(\lambda)/E(B\text{-}V)^{b}$
U	3600	4.9
B	4400	4.1
V	5500	3.1
R	6540	2.3
I	8060	1.5

[a]In Ångstroms, based on passbands of Bessell 1990.
[b]Based on values calculated from equations 2 and 3 of Cardelli et al. 1989.

not yield a consistent answer. In fact, the evidence seems to point to two disparate values. We adopt a reddening conversion $A_V=3.1\ E(B-V)$ for the following discussion (see Table 10). A list of all the reddening estimates we consider below appears in Table 11.

4.1 Material in the Milky Way

First, let us consider extinction due to material in the Milky Way itself in the direction of M81. The amount of H I in the Milky Way along the line of sight to M81 is small, leading Burstein & Heiles (1984) to conclude that the color excess is $E(B-V)=0.04$ mag. Kaufman *et al.* (1987) combine that estimate with three others and find a visual extinction in the foreground to M81 of $A_V\approx 0.3$ mag, which implies $E(B-V)\approx 0.1$ mag. However, these estimates are averages over large areas, and small-scale regions of higher and lower extinction are certainly present.

4.2 Measurements of Other Objects in M81

Several studies have been made of the extinction to individual objects in the disk of M81, including that due to foreground material as well as that due to the ISM in M81 itself. Kaufman *et al.* (1987) examined giant H II regions in M81 in the radio and concluded that the extinction varied somewhat over the face of the galaxy, but that the mean value was $A_V=1.0\pm 0.4$ mag. Hill *et al.* (1992) used the Ultraviolet Imaging Telescope to observe H II regions in the UV and concluded that A_V ranged from 1.0 to 1.5 mag, again varying from one place to another. Freedman *et al.* (1993) provide a measurement of the extinction to a number of Cepheids in M81 in two fields which are far from the position of SN 1993J. They find a difference between the reddening to Cepheids in M81 and in the LMC of

$$E(B-V)_{M81}-E(B-V)_{LMC}=-0.06 \text{ mag.}$$

Using their value of $E(B-V)_{LMC}=0.17$ mag implies a reddening of $E(B-V)_{M81}=0.11$ mag. Humphreys *et al.* (1986) found that *JHK* photometry of three M supergiants in M81 constrained the visual extinction to lie within the range $A_V=0.8-1.3$ mag. After the discovery of SN 1993J, Humphreys & Aldering (1993) measured *UBVR* values from photographic plates for stars within 20 arcsec of the SN. They found that the colors for three stars were distinctive enough to allow them to calculate the reddening, yielding values of $A_V=0.8$, 1.0, and 1.5 mag.

All these studies, except for that of Freedman *et al.* (1993), lead one to conclude that if SN 1993J suffers the same amount of internal extinction as other objects in M81, the total extinction is moderate, $A_V\approx 1.0$ mag, implying $E(B-V)\approx 0.32$ mag.

4.3 Observations of SN 1993J

On the other hand, most observations of SN 1993J itself may indicate a much smaller amount of extinction. Zimmerman *et al.* (1993) used x-ray data from *ROSAT* to estimate a column density of neutral hydrogen $N(\text{H I})=3.4\times 10^{20}$ cm^{-2} along the line of sight; using a relation of $N(\text{H I})=5.9\times 10^{21}\ E(B-V)$ mag cm^2 (Spitzer 1978), this implies $E(B-V)=0.06$ mag. On the basis of the strength of the 2200 Å absorption feature in the UV spectrum of SN 1993J, Wamsteker *et al.* (1993) suggested a similarly small value of $E(B-V)=0.07$ mag (although the wording of their announcement is somewhat ambiguous: they refer to the color excess $E(B-V)$ as "total extinction"). A more detailed analysis by Jeffery (1993) of

TABLE 11. Estimates of the reddening to SN 1993J.

Method	E(B-V) (mag)	Reference
due to Milky Way only		
HI col. density	0.04	Burstein & Heiles 1984
HI col. density, color of M81 nucleus		
Balmer decrement, IRAS 100 μm map	0.1	Kaufman et al. 1987
total: Milky Way plus M81		
M81 HII regions (radio)	0.32 ± 0.13	Kaufman et al. 1987
M81 HII regions (UV)	0.32 - 0.48	Hill et al. 1992
M81 Cepheids	0.11	Freedman et al. 1993
M81 M supergiants	0.26 - 0.42	Humphreys et al. 1986
M81 stars near SN 1993J	0.26 - 0.48	Humphreys & Aldering 1993
X-rays from SN 1993J	0.06	Zimmerman et al. 1993
UV continuum of SN 1993J	0.07	Wamsteker et al. 1993
UV continuum of SN 1993J	0.10 ± 0.03	Jeffery 1993
Na I equiv. widths	0.30 ± 0.10	this paper
Na I col. density	0.1 - 0.4	Wheeler et al. 1993
Na I col. density	0.2 - 0.5	this paper
early spectra of SN 1993J	0.15 ± 0.02	Wheeler et al. 1993
early colors of SN 1993J	0.13	Schmidt et al. 1993

the *IUE* spectra, using the UV extinction values of Cardelli *et al.* (1989), found that the strength of the 2200 Å feature yields $E(B-V)=0.10\pm0.03$ mag, and rules out a color excess of $E(B-V)\geqslant0.20$ mag. Both x-ray and UV observations of SN 1993J itself, then, suggest relatively little extinction, $A_V\approx0.25$ mag which implies $E(B-V)\approx0.08$ mag, roughly equal to the foreground extinction in the Milky Way alone.

As Humphreys (1993) has pointed out, however, the strength of the 2200 Å absorption feature may not be a reliable indicator of the visual extinction. Observations of the LMC (Nandy *et al.* 1980) show that the extinction in the UV below 2400 Å behaves differently than that in the Milky Way: the 2200 Å "bump" is smaller, and the extinction at shorter wavelengths increases much more steeply. Furthermore, several subsequent studies (Humphreys *et al.* 1984; Massey *et al.* 1985; Hutchings *et al.* 1987) indicate that the UV extinction in M31 and M33 behaves more like that of the LMC than that of the Milky Way. If the ISM in M81 has LMC-like properties, then it is possible that it could cause considerable extinction at UV and optical wavelengths without producing a telltale absorption feature at 2200 Å.

High-resolution optical spectroscopy of SN 1993J (Bowen *et al.* 1993) shows three systems of absorbing material: one due to material in M81, indicating that the supernova is affected by internal absorption, one due to the ISM of the Milky Way, and one at relatively large positive velocities ($v\approx120$ km/s), which may be caused by gas stripped from M82 (Yun *et al.* 1992). We present first a simple method to estimate the reddening from the observed Na I D-line equivalent widths, and then attempt to find the reddening from column densities of Na I.

The total equivalent widths of the Na I D lines, summing all three components, are $W_\lambda(D_1)=585$ mÅ and $W_\lambda(D_2)=799$ mÅ (Bowen *et al.* 1993). Sembach *et al.* (1993) provide high resolution Na I observations of 57 stars in the Milky Way, together with $E(B-V)$ values for each star. We compare their data with that of earlier authors (Hobbs 1969, 1974, 1976, 1978; Crutcher 1975; de Boer & Pottasch 1974) in Figs. 6(a) and 6(b). It is clear that the dataset of Sembach *et al.* (1993) samples stars with much larger equivalent widths; this may be due to the larger range of Galactic locations chosen for their study, which focused on long lines of sight through low density regions. Since the Sembach *et al.* (1993) data provide the only equivalent widths comparable to those measured in SN 1993J, we use their sample alone to make a linear fit to the relationship between Na I absorption and reddening. We find

$$E(B-V)=0.025+0.000454W_\lambda(D_1),$$

$$E(B-V)=0.015+0.000370W_\lambda(D_2),$$

where the widths are measured in mÅ. Applying these equations to the total Na I absorption in the line to sight to SN 1993J, we calculate reddenings $E(B-V)=0.29$ mag from the D_1 lines and $E(B-V)=0.31$ mag from the D_2 lines. These agree nicely with the "moderate" $E(B-V)$ $=0.32$ mag value, but the scatter among the points at such large equivalent widths is considerable; we place an uncertainty of 0.10 mag in these estimates. If we apply the above relationships to high resolution spectroscopy of SN 1987A in the LMC (Vidal-Madjar *et al.* 1987), we find that it predicts $E(B-V)=0.18$ mag, very close to the LMC reddening adopted by Freedman *et al.* (1993), but slightly larger than the value $E(B-V)=0.15$ mag adopted by Hamuy *et al.* (1988) to SN 1987A itself.

However, this simple analysis does not account for sat-

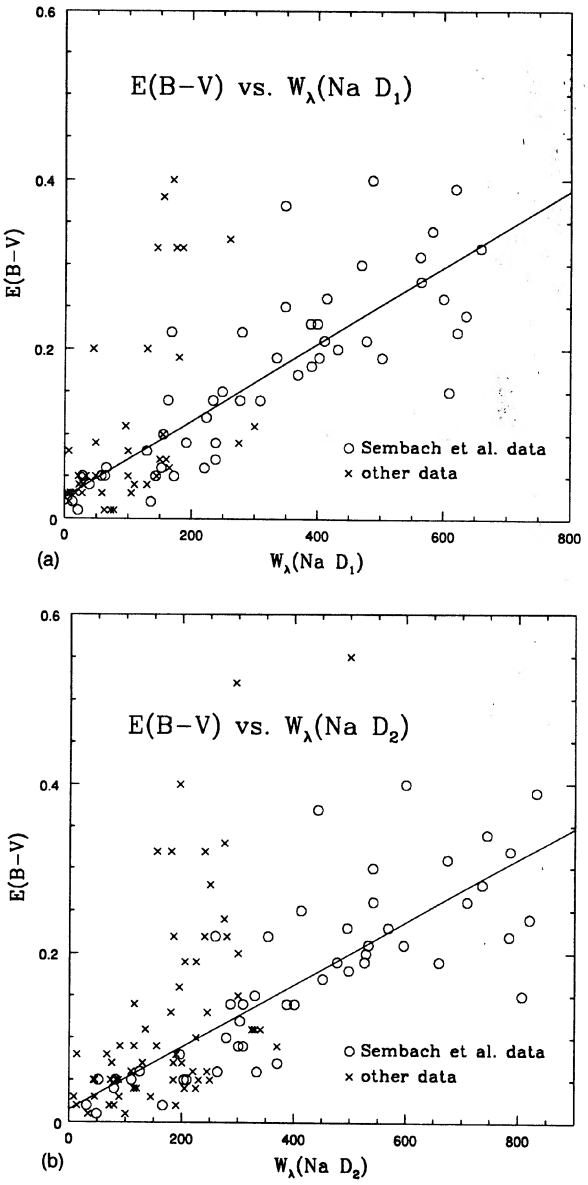

FIG. 6. (a) Comparison of reddening $E(B-V)$ vs equivalent width of Na I D_1 line. The line is a linear fit to the Sembach *et al.* (1993) data only (see Sec. 4.3). "Other data" refers to Hobbs (1969, 1974, 1976, 1978), Crutcher (1975), and de Boer & Pottasch (1974). (b) Comparison of reddening $E(B-V)$ vs equivalent width of Na I D_2 line. The line is a linear fit to the Sembach *et al.* (1993) data only (see Sec. *4.3*). "Other data" refers to Hobbs (1969, 1974, 1976, 1978), Crutcher (1975), and de Boer & Pottasch (1974).

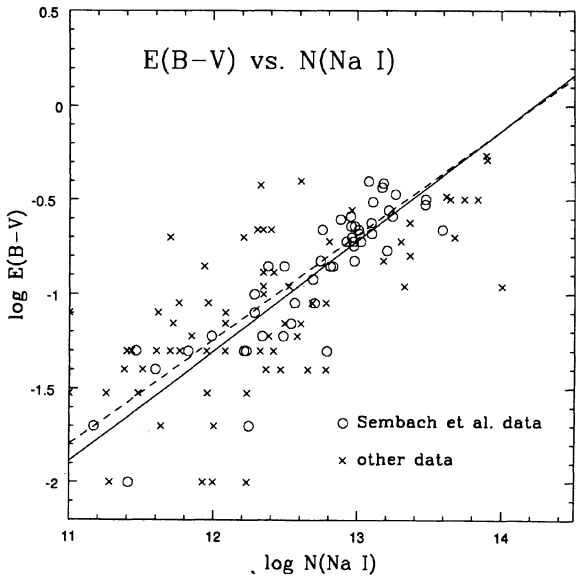

FIG. 7. Comparison of log E($B-V$) vs log (column density of Na I) derived from high-dispersion spectra. The solid line is a linear fit to the Sembach *et al.* (1993) data only, and the dashed line the relationship given in Hobbs (1974) which pertains to the "other" data only—taken from Hobbs (1969, 1974, 1976, 1978), Crutcher (1975), and de Boer & Pottasch (1974).

uration in the sodium lines, and one of the Milky Way components (at $v=-6$ km s^{-1}) is certainly saturated. Both Bowen *et al.* (1993) and Wheeler *et al.* (1993b) perform line-profile decomposition to calculate the column density of Na I atoms in the line of sight; while they agree that the Milky Way component is by far the largest, and that M81 contributes $N(\text{Na I})\approx 10^{13}$ cm^{-2}, they disagree on the total column density by a considerable factor. Bowen *et al.* (1993) conclude that $N(\text{Na I})_{\text{tot}}\approx 1.3\times 10^{14}$ cm^{-2}, while Wheeler *et al.* (1993b) state that $N(\text{Na I})_{\text{tot}}\approx 0.5\times 10^{14}$ cm^{-2}. We have attempted to find a relationship between the logarithms of Na I column density and color excess; see Fig. 7. We show the relation derived by Hobbs (1974), and one based solely on the Sembach *et al.* (1993) dataset. While the two linear fits are similar, they do not appear to predict E($B-V$) accurately for Na I column densities larger than about 10^{13} cm^{-2}. Moreover, there are only six stars with measured Na I column densities as large as the Wheeler *et al.* (1993b) value [all from the Crutcher (1975) and de Boer & Pottasch (1974) datasets], and none with a column density as large as the Bowen *et al.* (1993) figure. We suggest that this analysis indicates a reddening in the range E($B-V$)=0.2–0.5 mag, slightly larger than that given by Wheeler *et al.* (1993b), but hesitate to make any more precise claim.

It is possible, in theory, to derive the reddening from observations of the SN itself by assuming that it radiated as a blackbody during the first few days after the explosion, and fitting the observed colors to those of a reddened Planck spectrum. For example, Wheeler *et al.* (1993b) use spectra from March 31 and April 1 UT to find E($B-V$) $=0.15\pm 0.02$ mag, and Schmidt *et al.* (1993a) derive $A_V=0.4$ mag, which implies E($B-V$)=0.13 mag. Unfortunately, there are two complications in practice: First, it is necessary to have precise calibrations of the *absolute* flux corresponding to the zero-point of the magnitude scale in each passband in order to calculate the colors of a perfect blackbody. Second, the reddening vector in the ($U-B$) vs ($B-V$) plane, and that in ($B-V$) vs ($V-R$) plane, is almost exactly parallel to the roughly linear locus of points defined by blackbodies of various temperatures. Even if one uses only the earliest observations of SN 1993J [points at upper left in Fig. 8(a)], the observed ($U-B$) and ($B-V$) colors lie slightly on the "wrong" side of the blackbody locus—that is, they are more blue than an unreddened blackbody—and so cannot be due to a blackbody with any amount of extinction. It is possible that the SN did not exhibit a pure Planck spectrum even at these early times. In the ($B-V$) vs ($V-R$) plane, the earliest data are not inconsistent with the blackbody locus [see Fig. 8(b)], but do not reveal any preferred value for the reddening.

Since we cannot derive a definitive value for the extinction to SN 1993J, we will adopt two values for consideration in the remainder of this paper, representing the low [E($B-V$)=0.08 mag, $A_V=0.25$ mag] and moderate [E($B-V$)=0.32 mag, $A_V=1.0$ mag] possibilities. Note that the difference between the two is considerable: a factor of 2.0 in the V-band flux, 2.5 in B-band flux, and 4.0 in U-band flux.

5. ABSOLUTE MAGNITUDES

Once we choose a value for the reddening, we can calculate the absolute magnitude of SN 1993J in all colors (see Table 12). We adopt the distance modulus ($m-M$) $=27.8\pm 0.2$ mag to M81 derived by Freedman *et al.* (1993) from *HST* observations of Cepheids (based on a true distance modulus to the LMC of ($m-M$)=18.5 mag and a relatively low value for reddening to Cepheids in M81). Let us consider each of the two peaks in the light curve; the first, according to the visual estimates, occurred around March 30.7 UT. Since our CCD observations begin after that time (apart from one set of Leuschner 76 cm images taken through clouds), we can place only a rough lower limit on the luminosity of the SN at that time: $M_V\leqslant -17.4$, assuming E($B-V$)=0.08, or $M_V\leqslant -18.1$, assuming E($B-V$)=0.32. The second peak, on the other hand, was well covered by all our instruments. We find that the maximum brightness appears later at longer wavelengths. We list the observed values in each band, taking an unweighted average of the magnitudes from each observatory, in Table 12, together with the absolute magnitudes corresponding to the low and high values for extinction along the line of sight.

Is it possible to compare these absolute magnitudes with those of other SNe? One can try, but with little success. For example, since post-maximum spectra of SN 1993J seem similar to that of Type Ib SNe (Swartz *et al.* 1993; Filippenko *et al.* 1993), we have attempted to find absolute magnitudes of Type Ib SNe in the literature. However, we discovered three problems; first, there is surprisingly little

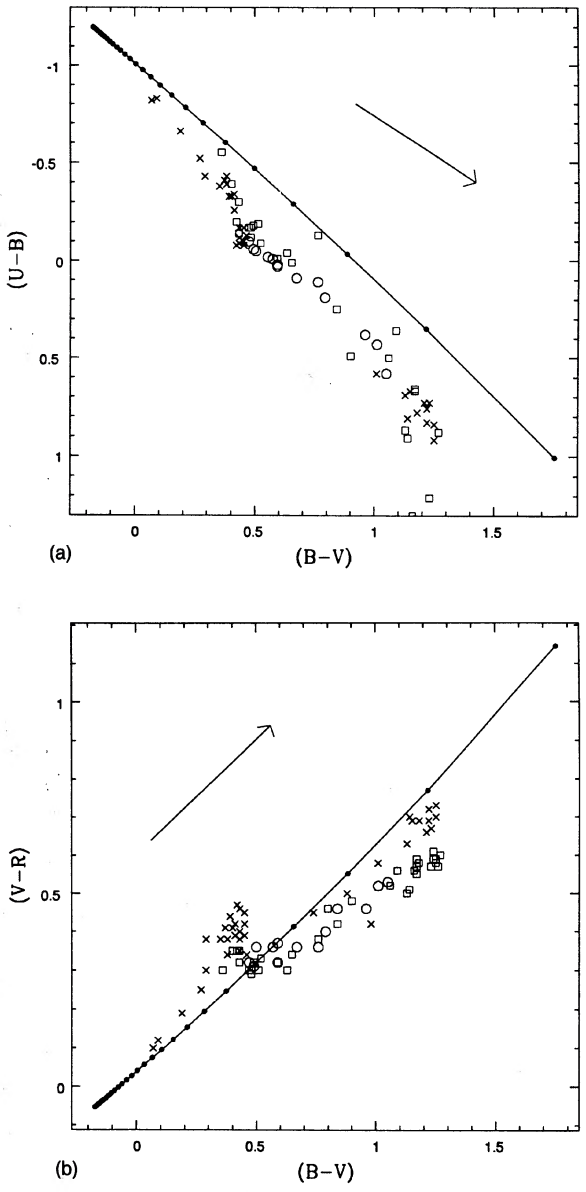

FIG. 8. (a) $(U-B)$ vs $(B-V)$ behavior of a blackbody and SN 1993J. The blackbody points start at $T=29\,000$ K at upper left and continue at decrements of 1000 K toward the lower right; the last point is $T=3000$ K. The SN 1993J points [symbols as in Fig. 4(a)] range from March 30.89 (upper left) to late May (lower right). The arrow shows how reddening of $E(B-V)=0.5$ mag would move a datum in the diagram. (b) $(V-R)$ vs $(B-V)$ behavior of a blackbody and SN 1993J. The blackbody points start at $T=29\,000$ K at lower left and continue at decrements of 1000 K toward the upper right; the last point is $T=3000$ K. The SN 1993J points [symbols as in Fig. 4(a)] range from March 30.89 (lower left) to late May (upper right). The arrow shows how reddening of $E(B-V)=0.5$ mag would move a datum in the diagram.

accurate published photometry for any Type Ib SN. Second, the corrections for extinction internal to host galaxies are always uncertain and, since Type Ib appear frequently near H II regions, probably not small. Finally, no Type Ib SN has occurred in a galaxy for which we have an accurate distance.

TABLE 12. Absolute magnitudes of SN 1993J.[a]

band	date of peak[b]	observed mag	absolute magnitude if $E(B-V)=0.08$	absolute magnitude if $E(B-V)=0.32$
U	9093.0	11.27 ±0.07	−16.90	−18.02
B	9093.7	11.35 ±0.05	−16.78	−17.75
V	9095.0	10.80 ±0.05	−17.25	−18.01
R	9095.3	10.47 ±0.03	−17.51	−18.06
I	9096.0	10.38 ±0.02	−17.54	−17.92

[a]At the secondary peak, and assuming $(m-M)=27.8$ (Freedman et al. 1993).
[b]JD - 2,440,000.

We have managed to find reasonable estimates for the absolute magnitude of three Type Ib SNe: 1983N, 1984L, and 1985F.[6]

In Table 13, we list M_B, or the closest equivalent, for each one, together with the assumptions entering the calculations. It appears that SN 1993J is less luminous than any of them, even after making a large correction for extinction. However, note that we have used $H_0=50$ km/s/Mpc to derive the values in Table 13; if we choose $H_0=75$ km/s/Mpc, the three Type Ib SNe would become 0.88 mag dimmer, and thus roughly equal to SN 1993J in M_B.

We can also attempt to compare SN 1993J with the only other known SN in the IIb class, SN 1987K in NGC 4651. Unfortunately, the amount of photometry for this object is very small; the list in Filippenko (1988) contains the only values we have been able to find in the literature. Most of these are determined from the integration of slit spectra, and have relatively large uncertainties. Moreover, all photometry (aside from the discovery image, which was unfiltered) is in a single color, roughly equivalent to the R bandpass. If we assume that the distance modulus to NGC 4651 is $(m-M)=30.8$ mag, appropriate[7] for a galaxy in the Virgo S cloud on the "others" scale (de Vaucouleurs 1993b), and assume further that the reddening to this SN was zero (Burstein & Heiles (1984) imply a Milky Way reddening of $E(B-V)<0.01$ mag), then the brightest observations of $m_R=14.2$ imply an absolute *R-band* magnitude $M_R=-16.6$. This value is much fainter than the range of values for SN 1993J, $-17.5>M_R>-18.1$, shown in Table 12. It is likely, however, that SN 1987K suffered from extinction internal to its host galaxy. Filippenko (1988) notes that the continuum of SN 1987K near maximum was slightly redder than that of SN 1987A; if the reddening to SN 1987K was $E(B-V)=0.20$ mag, slightly larger than that to SN 1987A, then the absolute magnitude for SN 1987K would be $M_R=-17.0$. Unfortunately, we cannot rule out even larger values of reddening within NGC 4651, or the possibility that observations of SN 1987K missed its actual maximum light. It is equally impossible to draw any meaningful comparison between the behavior of SN 1987K after maximum with that of SN 1993J: the data are simply too sparse and too imprecise.

It is clear that, without accurate photometry *and* distances *and* reddening measurements, it is impossible to

[6]Although no early-time specta of SN 1985F exist, its late-time spectrum resembles that of Type Ib/c SNe.

[7]Appropriate for the "others" scale, defined by de Vaucouleurs as "substantially independent of long- or short-scale prejudice."

TABLE 13. Absolute B magnitudes of SNe Ib.[a]

SN	galaxy	$m-M$	M_B	source	comments
1984L	NGC 991	32.5	≤ -18.1	Buta 1984	$A_B \approx 0.0$
1985F	NGC 4618	30.3	-18.2 to -19.7	Tsvetkov 1986	A_B very uncertain
1983N	NGC 5236	28.7	-17.7[b]	Panagia 1987	from IUE FES sensor

[a]Calculated using distances based on radial velocities for each galaxy from Sandage & Tammann 1987 and $H_0 = 50$ km/s/Mpc.
[b]The IUE FES passband peaks close to B, but extends much farther to the red, reaching well past 7000 Å (Holm & Crabb 1979).

make general statements about the homogeneity of absolute magnitudes of SNe.

6. BOLOMETRIC LIGHT CURVE

The true bolometric light curve of a supernova includes radiation from *all* wavelengths; it represents the total energy liberated in the explosion. Those who simulate SN explosions prefer to compare their models to bolometric luminosities, since they need not determine the exact distribution of flux across the spectrum. However, those who observe SNe can only measure the flux in a limited range of frequencies; they must add model-dependent "bolometric corrections," which supplement the observed flux, to their measurements. The resulting bolometric light curves are only as good as the assumptions entering the corrections.

We first, therefore, calculate the total observed optical (*UBVRI*) flux, which we call "quasibolometric," after Nomoto *et al.* (1990), in order to avoid any model dependencies. Note that the optical region does contain a significant fraction of the total energy emitted by a SN during the period near maximum visible light, starting several days after shock breakout. Adopting the magnitude–flux relationships of Bessell (1979; hereafter referred to as B79) and the passbands of Bessell (1990; hereafter referred to as B90) we show in Fig. 9 the fraction of the total energy described by Planck functions with various temperatures which falls within the optical range. The sum of *UBVRI* passbands contains over half the total flux from a blackbody with temperature 4000 K $< T <$ 11 000 K.

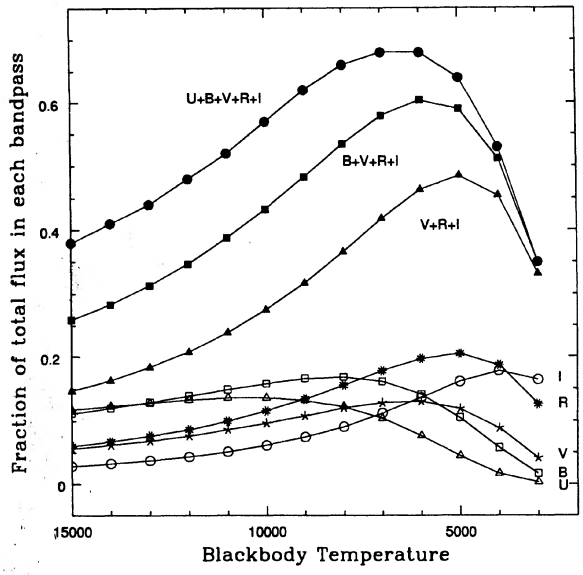

FIG. 9. Fraction of total blackbody flux emitted in Johnson–Cousins optical passbands, as a function of temperature. Calculations use the Bessell (1979) calibrations.

In order to convert the magnitudes of our light curves into fluxes, we need to adopt some set of conversion factors; this step can introduce important systematic differences between objects and between observers. The conversion depends on the shape of the effective passbands, absolute spectrophotometry of some star, and a zero-point correction to correct for the difference between the standard system colors of that star and the actual ratio of fluxes observed in the passbands. We adopt the B79 conversion factors, and point out to the reader that these factors are crucial in determining temperatures and bolometric fluxes. When adding together the flux from adjoining bands, we have made a small adjustment to eliminate the energy which is "counted twice" because it falls into the region of overlap between filters. Using the B90 bandpasses, we find for an object with a flat spectrum

(true flux across *UBVRI*)
$= 0.945$(sum of *UBVRI* fluxes).

In Fig. 10 and Table 14 (column 2) (this table is presented in its complete form in the ApJ/AJ CD-ROM Series, Vol. 2, 1994), we give the fluxes corresponding to our measured light curves, using the sum of *UBVRI* where possible. We have included points calculated from *BVRI* measurements, without *U*, at late times, when *U*-band measurements are sparse and uncertain. This introduces only a small systematic difference, since after May 25 the *U*-band flux amounts to less than three percent of the total *UBVRI* sum.

Of course, the flux we detect depends very sensitively on the amount of extinction along the line of sight to the SN. Moreover, since extinction is strongly color dependent, and since the SN changed color sharply during the first few weeks, the correction is not constant: the ratio by which we must multiply the optical flux changes by almost a factor of two over the period of our observations. Using the interstellar extinction values shown in Table 10,[8] we correct the fluxes for extinction corresponding to low [$E(B$

[8]These values are based on the measurements of Cardelli *et al.* (1989) in the Milky Way; recall that extinction in the *visible* does not differ much between the Milky Way and the LMC, and, presumably, M81.

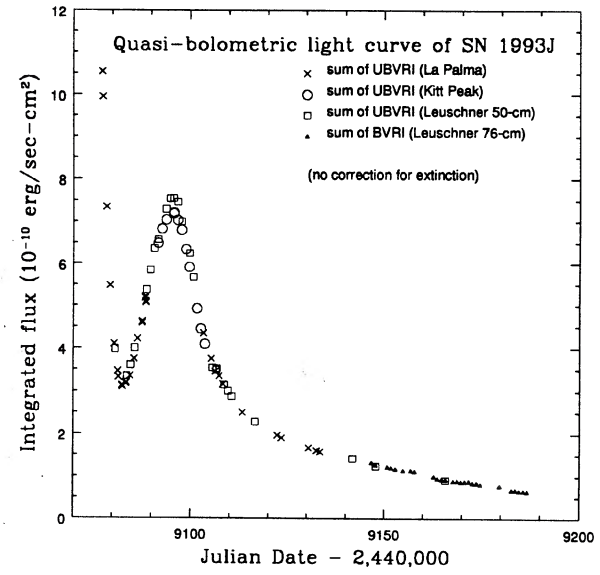

FIG. 10. Sum of observed optical fluxes ("quasibolometric" light curve), using the magnitude/flux relation of Bessell (1979).

$-V)=0.08$ mag] and moderate [$E(B-V)=0.32$ mag] values of the total reddening to SN 1993J, and list the corrected fluxes in columns 3 and 4 of Table 14, respectively.

By making a set of additional assumptions, we can calculate the bolometric luminosity of SN 1993J. First, for each of the possible reddening values, we correct the observed *UBVRI* fluxes and then find the temperature of a blackbody which best fits each observation (see Fig. 11 and Table 15; this table is presented in its complete form in the

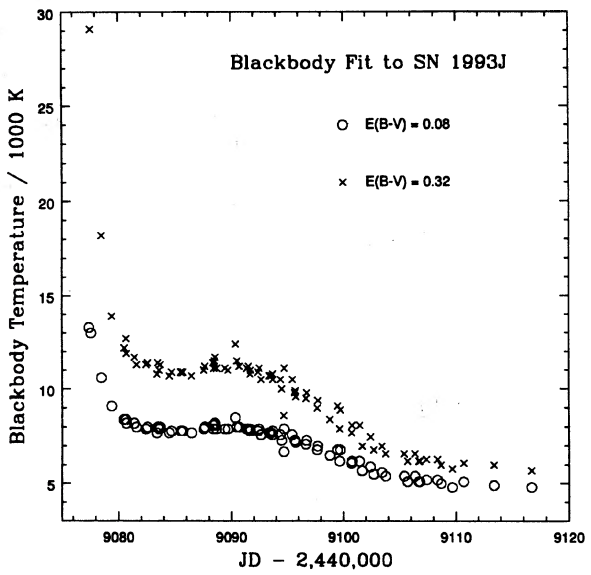

FIG. 11. Blackbody fits to the colors of SN 1993J in *UBVRI*, using the flux–mag relationship of Bessell (1979), for two values of reddening $E(B-V)$. All temperatures are integral multiples of 100 degrees.

TABLE 14. Summed optical fluxes[a] of SN 1993J.*

	corrected for extinction				
JD[b]	observed	E(B-V)=0.08	E(B-V)=0.32	site[c]	bands
9077.39	1.054e-09	1.384e-09	4.351e-09	LP	UBVRI
9077.56	9.950e-10	1.305e-09	4.089e-09	LP	UBVRI
9078.48	7.348e-10	9.544e-10	2.882e-09	LP	UBVRI
9079.40	5.481e-10	7.061e-10	2.065e-09	LP	UBVRI
9080.49	4.104e-10	5.259e-10	1.508e-09	LP	UBVRI
9080.70	3.978e-10	5.100e-10	1.465e-09	L	UBVRI
9081.40	3.469e-10	4.427e-10	1.248e-09	LP	UBVRI
9081.59	3.331e-10	4.251e-10	1.199e-09	LP	UBVRI
9082.45	3.137e-10	4.002e-10	1.126e-09	LP	UBVRI
9082.58	3.109e-10	3.963e-10	1.113e-09	LP	UBVRI
9083.41	3.185e-10	4.053e-10	1.127e-09	LP	UBVRI
9083.47	3.179e-10	4.044e-10	1.124e-09	LP	UBVRI
9083.60	3.203e-10	4.075e-10	1.133e-09	LP	UBVRI
9083.70	3.347e-10	4.270e-10	1.201e-09	L	UBVRI
9084.49	3.356e-10	4.262e-10	1.176e-09	LP	UBVRI
9084.70	3.607e-10	4.591e-10	1.279e-09	L	UBVRI
9085.52	3.753e-10	4.763e-10	1.309e-09	LP	UBVRI
9085.60	3.757e-10	4.771e-10	1.314e-09	LP	UBVRI
9085.70	4.000e-10	5.087e-10	1.409e-09	L	UBVRI
9086.48	4.223e-10	5.358e-10	1.471e-09	LP	UBVRI
9087.57	4.589e-10	5.831e-10	1.607e-09	LP	UBVRI
9087.66	4.622e-10	5.874e-10	1.620e-09	LP	UBVRI
9088.39	5.179e-10	6.564e-10	1.790e-09	LP	UBVRI
9088.43	5.213e-10	6.604e-10	1.799e-09	LP	UBVRI
9088.51	5.097e-10	6.464e-10	1.767e-09	LP	UBVRI
9088.56	5.066e-10	6.421e-10	1.752e-09	LP	UBVRI
9088.70	5.366e-10	6.826e-10	1.890e-09	L	UBVRI
9089.70	5.845e-10	7.434e-10	2.058e-09	L	UBVRI
9090.70	6.357e-10	8.089e-10	2.243e-09	L	UBVRI
9091.67	6.490e-10	8.243e-10	2.267e-09	KP	UBVRI
9091.70	6.568e-10	8.351e-10	2.307e-09	L	UBVRI
9092.65	6.827e-10	8.662e-10	2.372e-09	KP	UBVRI
9093.69	7.044e-10	8.923e-10	2.428e-09	KP	UBVRI
9093.70	7.292e-10	9.269e-10	2.560e-09	L	UBVRI
9094.70	7.536e-10	9.563e-10	2.620e-09	L	UBVRI
9095.65	7.192e-10	9.086e-10	2.443e-09	KP	UBVRI
9095.70	7.543e-10	9.537e-10	2.572e-09	L	UBVRI
9095.74	7.215e-10	9.115e-10	2.450e-09	KP	UBVRI
9096.65	7.031e-10	8.868e-10	2.369e-09	KP	UBVRI
9096.70	7.455e-10	9.427e-10	2.543e-09	L	UBVRI
9097.65	6.798e-10	8.552e-10	2.257e-09	KP	UBVRI
9097.70	6.997e-10	8.824e-10	2.353e-09	L	UBVRI
9098.78	6.341e-10	7.953e-10	2.073e-09	KP	UBVRI
9099.65	5.915e-10	7.393e-10	1.898e-09	KP	UBVRI
9099.70	6.243e-10	7.853e-10	2.076e-09	L	UBVRI
9100.70	5.672e-10	7.075e-10	1.799e-09	L	UBVRI
9101.65	4.922e-10	6.104e-10	1.513e-09	KP	UBVRI
9102.67	4.448e-10	5.500e-10	1.345e-09	KP	UBVRI
9103.41	4.345e-10	5.364e-10	1.301e-09	LP	UBVRI
9103.75	4.096e-10	5.055e-10	1.224e-09	KP	UBVRI
9105.41	3.759e-10	4.621e-10	1.099e-09	LP	UBVRI
9105.70	3.545e-10	4.358e-10	1.035e-09	L	UBVRI
9106.37	3.459e-10	4.247e-10	1.004e-09	LP	UBVRI
9106.70	3.490e-10	4.288e-10	1.019e-09	L	UBVRI
9106.80	3.522e-10	4.328e-10	1.028e-09	L	UBVRI
9107.40	3.358e-10	4.117e-10	9.664e-10	LP	UBVRI
9108.38	3.170e-10	3.883e-10	9.085e-10	LP	UBVRI
9108.70	3.142e-10	3.849e-10	9.001e-10	L	UBVRI
9109.70	3.005e-10	3.677e-10	8.545e-10	L	UBVRI
9110.70	2.872e-10	3.524e-10	8.327e-10	L	UBVRI

*Table 14 is also presented in its complete form in the ApJ/AJ CD-ROM Series, Vol. 2, 1994.

ApJ/AJ CD-ROM Series, Vol. 2, 1994). Note that the assumed reddening makes a very large difference in fitted temperature at very early times. We remind the reader that there may be systematic errors in our calculations of fluxes which would affect the derived temperatures. Having found the temperature corresponding to each set of optical fluxes, we determine the fraction of the blackbody flux

TABLE 15. Blackbody temperature and luminosity[a] of SN 1993J.*

	$E(B-V)=0.08$		$E(B-V)=0.32$			
JD	Temp	Luminosity	Temp	Luminosity	site[c]	bands
9077.39	13300	5.07	31100	38.07	LP	UBVRI
9077.56	13000	4.67	29100	33.90	LP	UBVRI
9078.48	10600	2.78	18200	15.13	LP	UBVRI
9079.40	9100	1.82	13900	7.93	LP	UBVRI
9080.49	8400	1.29	12200	5.05	LP	UBVRI
9080.70	8200	1.24	11900	4.81	L	UBVRI
9081.40	8200	1.07	11700	4.01	LP	UBVRI
9081.59	8000	1.01	11300	3.70	LP	UBVRI
9082.45	7900	0.95	11300	3.48	LP	UBVRI
9082.58	8000	0.95	11400	3.44	LP	UBVRI
9083.41	7700	0.95	10800	3.35	LP	UBVRI
9083.47	8000	0.96	11400	3.47	LP	UBVRI
9083.60	7900	0.97	11000	3.43	LP	UBVRI
9083.70	8000	1.02	11300	3.71	L	UBVRI
9084.49	7700	1.00	10700	3.43	LP	UBVRI
9084.70	7800	1.10	10900	3.80	L	UBVRI
9085.52	7800	1.14	10900	3.89	LP	UBVRI
9085.60	7800	1.14	10900	3.90	LP	UBVRI
9085.70	7800	1.21	10900	4.19	L	UBVRI
9086.48	7700	1.26	10700	4.29	LP	UBVRI
9087.57	7900	1.39	11000	4.87	LP	UBVRI
9087.66	8000	1.40	11200	5.00	LP	UBVRI
9088.39	8100	1.59	11400	5.53	LP	UBVRI
9088.43	7900	1.58	11100	5.45	LP	UBVRI
9088.51	8100	1.57	11500	5.57	LP	UBVRI
9088.56	8200	1.56	11700	5.63	LP	UBVRI
9088.70	7900	1.63	11100	5.72	L	UBVRI
9089.70	7900	1.77	11000	6.23	L	UBVRI
9090.70	8000	1.93	11200	6.93	L	UBVRI
9091.67	7800	1.97	10800	6.74	KP	UBVRI
9091.70	7900	1.99	11000	6.99	L	UBVRI
9092.65	7600	2.04	10500	6.79	KP	UBVRI
9093.69	7600	2.10	10500	6.95	KP	UBVRI
9093.70	7800	2.21	10800	7.61	L	UBVRI
9094.70	7900	2.28	11100	7.94	L	UBVRI
9095.65	7300	2.10	9800	6.63	KP	UBVRI
9095.70	7300	2.21	9900	7.11	L	UBVRI
9095.74	7200	2.11	9600	6.54	KP	UBVRI
9096.65	7100	2.05	9500	6.32	KP	UBVRI
9096.70	7300	2.18	9800	6.91	L	UBVRI
9097.65	6800	1.95	9000	5.73	KP	UBVRI
9097.70	7000	2.04	9400	6.18	L	UBVRI
9098.78	6500	1.81	8400	5.10	KP	UBVRI
9099.65	6200	1.71	7900	4.53	KP	UBVRI
9099.70	6800	1.79	8900	5.27	L	UBVRI
9100.70	6100	1.64	7700	4.23	L	UBVRI
9101.65	5700	1.44	7000	3.50	KP	UBVRI
9102.67	5500	1.29	6800	3.07	KP	UBVRI
9103.41	5600	1.26	7000	3.01	LP	UBVRI
9103.75	5400	1.21	6600	2.79	KP	UBVRI
9105.41	5400	1.10	6600	2.51	LP	UBVRI
9105.70	5100	1.07	6200	2.40	L	UBVRI
9106.37	5400	1.01	6600	2.29	LP	UBVRI
9106.70	5100	1.05	6200	2.36	L	UBVRI
9106.80	5100	1.06	6200	2.38	L	UBVRI
9107.40	5200	1.00	6300	2.21	LP	UBVRI
9108.38	5200	0.94	6300	2.07	LP	UBVRI
9108.70	5000	0.95	6000	2.08	L	UBVRI
9109.70	4800	0.93	5800	1.98	L	UBVRI
9110.70	5100	0.87	6100	1.93	L	UBVRI
9113.39	4900	0.76	6000	1.64	LP	UBVRI
9116.70	4800	0.71	5700	1.52	L	UBVRI
9122.40	4800	0.61	5800	1.29	LP	UBVRI
9123.40	4800	0.59	5800	1.25	LP	UBVRI
9130.38	4900	0.51	5900	1.11	LP	UBVRI
9132.41	4800	0.50	5800	1.06	LP	UBVRI
9133.38	4800	0.49	5800	1.05	LP	UBVRI
9141.80	5000	0.43	6000	0.97	L	UBVRI
9147.80	4900	0.38	5900	0.85	L	UBVRI
9165.70	5100	0.28	6200	0.64	L	UBVRI
9147.70	5300	0.40	6600	0.94	L	BVRI
9150.70	5300	0.39	6600	0.91	L	BVRI
9151.70	5400	0.38	6700	0.90	L	BVRI
9152.80	5300	0.37	6600	0.88	L	BVRI
9154.80	5400	0.36	6700	0.85	L	BVRI
9156.80	5600	0.36	7100	0.87	L	BVRI
9157.80	5600	0.35	7100	0.85	L	BVRI
9162.70	5500	0.32	6900	0.77	L	BVRI
9163.70	5500	0.30	6900	0.73	L	BVRI
9164.70	5400	0.30	6800	0.71	L	BVRI
9165.70	5400	0.29	6700	0.70	L	BVRI
9167.70	5400	0.28	6700	0.67	L	BVRI
9168.70	5500	0.28	6900	0.68	L	BVRI
9169.70	5600	0.28	7100	0.67	L	BVRI
9170.70	5600	0.28	7000	0.67	L	BVRI
9171.70	5800	0.28	7500	0.71	L	BVRI
9172.70	5700	0.26	7300	0.66	L	BVRI
9173.70	5700	0.26	7200	0.66	L	BVRI
9174.70	5700	0.25	7300	0.64	L	BVRI
9179.70	5900	0.24	7600	0.63	L	BVRI
9182.70	5600	0.22	7100	0.52	L	BVRI
9183.70	5800	0.21	7400	0.55	L	BVRI
9184.70	5700	0.21	7200	0.52	L	BVRI
9185.70	5900	0.21	7700	0.54	L	BVRI
9186.70	5800	0.20	7400	0.52	L	BVRI

[a] In units of 10^{42} erg cm^{-2} s^{-1}. Assumes distance to M81 is 3.63 Mpc.
[b] Julian Day - 2,440,000.
[c] LP = La Palma; KP = Kitt Peak; L = Leuschner.

*Table 15 is also presented in its complete form in the ApJ/AJ CD-ROM Series, Vol. 2, 1994.

emitted outside the *UBVRI* window and add it to the observed amount. Note that since the estimated blackbody temperature stays within the range 5000–11 000 K, after the initial minimum, the ratio of blackbody flux to *UBVRI* flux is constant to within about 20 percent (see Fig. 9). Finally, adopting the distance modulus of $(m-M)=27.8$ mag determined to M81 by Freedman *et al.* (1993), we convert these fluxes into luminosities. We list the bolometric luminosity of SN 1993J derived in this manner in Table 15, and plot the bolometric light curves in Fig. 12.

Note that the difference between the two curves in Fig. 12 is not a constant; it decreases from a factor of ~ 6 at early times to only ~ 2.5 on the exponential tail. A larger reddening value implies a stronger correction to the *U* and *B* fluxes, which at early times leads to a much higher temperature; the higher temperature, in turn, implies a larger bolometric correction. At late times, when the *R* and *I* fluxes dominate, and when the temperature changes much more slowly, different values for the reddening yield luminosities with an almost constant offset. For example, the rate of decline on the exponential tail (after May 22), based on *BVRI* measurements, is 0.019 and 0.018 mag per day for low and high values of $E(B-V)$, respectively. Both rates are much faster than that due to the decay of ^{56}Co, which is only 0.0098 mag per day; we interpret this as evidence that some gamma rays are escaping directly from the interior of the ejecta, due to the small mass of the hydrogen envelope (Leibundgut & Pinto 1992). The very fast decline provides no evidence for the presence of a pul-

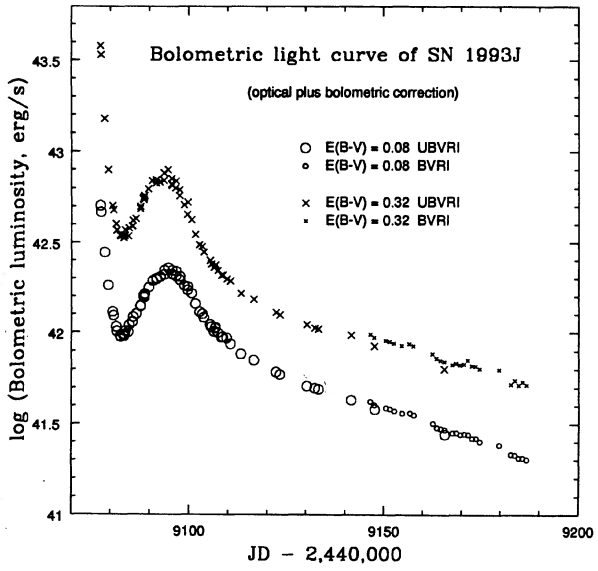

FIG. 12. Bolometric luminosity of SN 1993J, for two values of reddening $E(B-V)$, assuming distance to M81 is 3.63 Mpc (Freedman *et al.* 1993) and assuming the supernova radiates as a perfect blackbody.

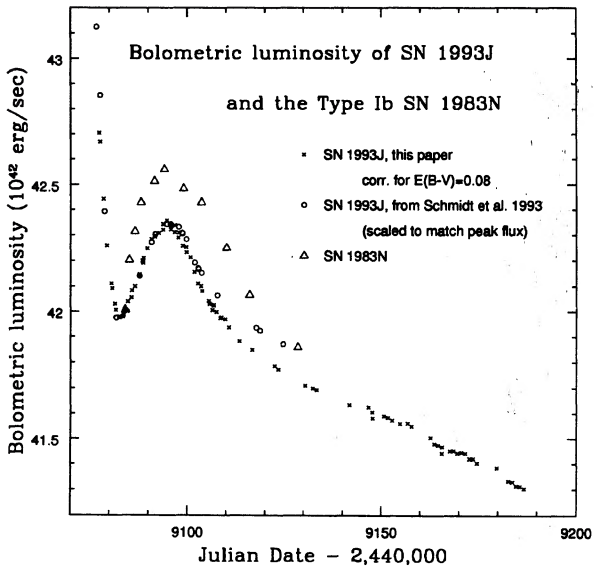

FIG. 13. Comparison of the bolometric light curve of the Type Ib SN 1983N with that of SN 1993J. The 1983N points (Nomoto 1993) have been shifted in time to match the secondary peak of SN 1993J, and assume a distance of 5.5 Mpc for NGC 5236. We also plot the bolometric curve of SN 1993J from Schmidt *et al.* (1993), which has been scaled in flux to match our curve at the secondary peak.

sar or other additional energy source in the remnant, but agrees with the models of Woosley *et al.* (1993).

7. COMPARISON WITH THE TYPE Ib SN 1983N

SN 1993J represents a link between the supernova Types II and Ib: there are strong grounds for believing that, if the progenitor had managed to lose the small amount of hydrogen left in its envelope, the event would have been classified as a normal Type Ib (Nomoto *et al.* 1993; Podsiadlowski *et al.* 1993; Woosley *et al.* 1993; Filippenko & Matheson 1993a). Therefore, SN 1993J is therefore best classified as a Type IIb (Woosley *et al.* 1987). The spectra of SN 1993J from late April ($t \approx 30$ days) and later times are similar to those of a Type Ib, although hydrogen could still be seen through 1993 September (Filippenko & Matheson 1993b). We expect that the *bolometric* evolution of SN 1993J should not be altered greatly by the small shell of hydrogen [$\mathcal{M}(\mathrm{H}) \approx 0.15\,\mathcal{M}_\odot$] remaining at the surface, although the precise distribution of energy across the optical region obviously is affected. Therefore, we might expect the bolometric light curve of SN 1993J to resemble that of a Type Ib SN. Panagia (1987) has created a nearly bolometric light curve for the prototypical Type Ib SN 1983N by combining *IUE* spectra and optical and *JHK* photometry [assuming $E(B-V)=0.16$ mag], covering a period from roughly seven to fifty days after the explosion. In Table 16 we list this light curve for SN 1983N, and in Fig. 13 compare it with our own bolometric estimates for SN 1993J, after correcting for reddening of $E(B-V)=0.08$ mag to the latter.

TABLE 16. SN 1983N.[a]

Day[b]	flux[c]
6.0	2.8
7.0	4.4
8.5	5.7
10.0	7.4
13.5	9.0
16.0	10.0
21.0	8.4
25.5	7.4
32.0	4.9
38.0	3.2
50.5	2.0

[a]From Nomoto 1993.
[b]Time since 1983, June 28.
[c]In units of 10^{-10} erg cm^{-2} s^{-1}.

The comparison reveals a fair similarity between the two supernovae, as Nomoto *et al.* (1993) noted. The secondary maximum in the SN 1993J light curve has roughly the same width and height, relative to the late-time tail, as SN 1983N. The rise to peak luminosity seems to be similar, although we lack data for the shock-heated phase of SN 1983N. A closer look, however, reveals that the SN 1993J peak declines more sharply than that of SN 1983N, dropping by a factor of two from maximum within only seven days. SN 1983N took twice as long, about fifteen days, to fade by the same factor. As Fig. 13 shows, Schmidt *et al.* (1993a) derive a bolometric light curve for SN 1993J which drops *less* sharply than ours, especially at the "knee" in the light curve. The difference between their calculations and ours is largely in the bolometric correction: we assume that SN 1993J radiates as a perfect blackbody (an approximation which grows less accurate at late times), whereas Schmidt *et al.* (1993a) make a more com-

plex set of corrections (see Schmidt *et al.* 1993b). In any case, we conclude that the shape of the bolometric light curve of SN 1993J is not greatly different from that of SN 1983N.[9] It is especially unfortunate that we have no information along the exponential tail of SN 1983N, since the spectrum of SN 1993J is apparently in the process of growing very similar to that of a Type Ib in the nebular phase (Filippenko *et al.* 1993).

For curiosity's sake, we can try to compare the absolute luminosity at the secondary peak of SN 1993J with that of SN 1983N at its peak. Unfortunately, the distance to the host galaxy of the latter, NGC 5236=M83, is rather uncertain. We have not been able to find any recent measurements, and the older literature supplies values ranging from 3.7 Mpc (de Vaucouleurs 1979) to 8 Mpc (Sandage & Tammann 1974). Using these two as lower and upper limits, and adopting a peak exoatmospheric flux of 10^{-9} erg cm^{-2} s^{-1}, we find that the luminosity of SN 1983N was $(1.6\text{–}7.7)\times10^{42}$ erg s^{-1}. The main uncertainty in the luminosity of SN 1993J, on the other hand, is due to the unknown extinction along the line of sight. Using a distance of 3.63 Mpc for M81 and the two values $E(B-V)=0.08$ and $E(B-V)=0.32$ mag for reddening, the range of the luminosity of SN 1993J at its second peak is $(2.0\text{–}6.3)\times10^{42}$ ergs s^{-1}. We conclude that the two supernovae were certainly comparable in brightness, to within a factor of two or so.

In summary, while there are small differences between the two light curves, it appears that the total luminosity of SN 1993J varied with time in a manner similar to that of SN 1983N, lending support to the idea that the explosion mechanism and progenitor structure of SN 1993J may have been very similar to that of Type Ib SNe.

8. CONCLUSIONS

Our attempt to merge photometry from three different sites and five different telescopes succeeds in yielding consistent, detailed light curves of SN 1993J in the optical, starting within three days of the likely time of core collapse and continuing for over one hundred days. However, the unknown amount of extinction along the line of sight to the SN complicates their interpretation; there is conflicting evidence for small [$E(B-V)\approx0.08$ mag] and moderate [$E(B-V)\approx0.32$ mag] values for the reddening. Nonetheless, we can state with some confidence that the optical behavior of SN 1993J after its envelope became optically thin resembles that of SN 1987A in showing an exponential decrease in brightness which is progressively more rapid at long wavelengths. The rate of decline, however, is considerably faster than that of SN 1987A, and faster than that produced by the radioactive decay of ^{56}Co. We have calculated the evolution of the total optical ($UBVRI$) flux, and have estimated the bolometric light curve as well. A comparison of the bolometric light curve with that of the Type Ib SN 1983N shows that the two events were similar, lending support to the hypothesis that the progenitors of Type Ib SNe are massive stars which have lost all of their hydrogen envelope before the core collapses.

[9]We suspect that the wider spectral coverage of SN 1983N, especially in the infrared, leads to significant differences in bolometric calculations at late times.

The observations in this paper sample only a small fraction of the enormous mass of contributions which were shared unselfishly by researchers around the world via electronic networks. We thank Bjorn H. Granslo, Taichi Kato, Guy Hurst, and especially Ralph A. M. J. Wijers for their electronic compilations of optical and near-IR observations. Harold Corwin's photometry gave us a great head start in making light curves. Brian Schmidt and Nick Suntzeff provided much-needed expertise in creating bolometric light curves, and Brian supplied us with the nice image of M81 that appears as Fig. 1. Gerard de Vaucouleurs contributed many useful bits of information on M81 and the field around SN 1993J, and made several suggestions which have improved the quality of our photometry. We thank Janet A. Mattei for sending us observations of SN 1991T from the AAVSO international data base. David Bowen and his coauthors supplied a copy of their paper on high resolution spectral measurements of SN 1993J in advance of its publication, which helped our analysis of the reddening. Ralph Martin, Jim Lewis, and a host of observers at Royal Greenwich Observatory very generously made their data freely available to all via FTP. We are grateful to Sun Microsystems Inc. (Academic Equipment Grant Program) and to Photometrics Ltd. for equipment donations that were vital to the acquisition and reduction of data at Leuschner Observatory. Financial support for this research was provided to A.V.F. through NSF Grant Nos. AST-8957063 and AST-9115174, CalSpace Grant No. CS-96-91, and the Center for Particle Astrophysics (NSF Cooperative Agreement No. AST-8809616). The contributions of our friend and colleague Alain C. Porter to the study of SN 1993J and other supernovae were cut short by his untimely death on October 10, 1993. We will miss his enthusiasm and his courage. Requiescat in pace.

APPENDIX: REDUCTION OF LEUSCHNER DATA

We performed the following steps for each night of observations. During the early afternoon, we created a master bias frame by taking the median, pixel by pixel, of five individual bias frames. We then created a master dark-current frame by taking the median of five exposures with the camera's shutter closed, each ten minutes long. At sunset, we took a series of five exposures of the twilight sky through each filter and created a flatfield frame by taking the median of the bias-subtracted, dark-subtracted images. During the night, we subtracted the master bias frame from each new image, subtracted a copy of the master dark frame (scaled to match the image's exposure length) and divided by the appropriate flatfield frame. On the infrequent occasions when the weather prevented us from obtaining sky flats at sunset, we used flatfield frames from the most recent evening.

We extracted aperture magnitudes from each image using the IMEXAM task in IRAF,[10] and found the difference between the instrumental magnitudes of SN 1993J and star B. We then made a correction to the raw *B*-band differential magnitudes *only* to account for color-dependent extinction as follows. Let b_{SN} and b_B denote the raw, instrumental magnitudes of the SN and star B in *B*-band, and v_{SN} and v_B those in *V* band. Define $\Delta b = b_{SN} - b_B$, and $\Delta v = v_{SN} - v_B$. We then calculate a value for the difference in *B*-band brightness between the SN and star B which incorporates the different amounts of atmospheric extinction they suffer due to their different colors,

$$(b_{SN} - b_B)^0 = \Delta b - k''_{bv} X (\Delta b - \Delta v),$$

where X is the airmass of each observation. We used a value $k''_{bv} = 0.033$, taken from calculations based on the Johnson–Cousins filter system and properties of the atmosphere (de Vaucouleurs 1993a), which is close to the value 0.03 derived observationally by Montgomery *et al.* (1993) using Landolt standards at Kitt Peak. We then used the corrected differential magnitude $(b_{SN} - b_B)^0$ in all further calculations, and indicate this corrected value by b^0 below.

In order to transform the differential instrumental magnitudes to the Johnson–Counsins system, we applied color corrections based on observations of the M67 "dipper" asterism (described in Schild 1983, among others), using photometry supplied by Porter (1993), and the field around PG 1633+009, using photometry of Landolt (1992). Our transformations from instrumental magnitudes (lower case) to standard values (upper case) were, for the 50 cm data,

$$R = r + 0.30(r-i) + C_R,$$
$$(V-R) = 0.82(v-r) + C_V,$$
$$(B-V) = 1.10(b^0-v) + C_B,$$
$$(U-B) = 1.10(u-b^0) + C_U,$$
$$(R-I) = 1.17(r-i) + C_I,$$

and for the 76 cm data,

$$R = r + 0.27(r-i) + C_R,$$
$$(V-R) = 0.86(v-r) + C_V,$$
$$(B-V) = 1.13(b^0-v) + C_B,$$
$$(U-B) = 1.86(u-b^0) + C_U,$$
$$(R-I) = 1.28(r-i) + C_I.$$

The constants C_R, C_V, etc., were chosen individually in each image to bring the magnitude of star B to the Corwin value (see Table 1). Thus, we essentially performed differential photometry between the SN and star B, including first-order color terms.

Note the large value for the $(U-B)$ coefficient of the 76 cm data; it is one indication that the *U* passband of the 76 cm telescope is far from the standard Johnson *U*. As mentioned in the text, we therefore use the 76 cm *U*-band values only for qualitative purposes.

[10]IRAF is maintained and distributed by the National Optical Astronomy Observatory.

REFERENCES

Aldering, G., Humphreys, R. M., & Richmond, M. W. 1994, AJ (in press)
Bessell, M. S. 1979, PASP, 91, 589 (B79)
Bessell, M. S. 1990, PASP, 102, 1181 (B90)
Bowen, D. V., Roth, K. C., Blades, J. C., & Meyer, D. M. 1993, ApJL (submitted)
Burstein, D., & Heiles, C. 1984, ApJS, 54, 33
Buta, R. 1984, IAU Circ. No. 3981
Calamai, G., Govazzi, G., Randone, I., & Tofani, G. 1993, IAU Circ. No. 5741
Cardelli, J. A., Clayton, G. C., & Mathis, J. S. 1989, ApJ, 345, 245
Corwin, H. G. 1993, IAU Circ. No. 5742
Crutcher, R. M. 1975, ApJ, 202, 634
de Boer, K. S., & Pottasch, S. R. 1974, A&A, 32, 1
de Vaucouleurs, G. 1979, ApJ, 227, 729
de Vaucouleurs, G. 1993a, private communication
de Vaucouleurs, G. 1993b, ApJ, 415, 10
Filippenko, A. V. 1988, AJ, 96, 1941
Filippenko, A. V., Bower, G. C., Barth, A. J., Ho, L. C., Stringfellow, G. S., Goodrich, R. W., & Porter, A. C. 1994, in preparation
Filippenko, A. V., & Matheson, T. 1993a, IAU Circ. No. 5787
Filippenko, A. V., & Matheson, T. 1993b, private communication
Filippenko, A. V., Matheson, T., & Ho, L. C. 1993, ApJ, 415, L103
Filippenko, A. V., Treffers, R. R., Paik, Y., Davis, M., & Schlegel, D. 1993, IAU Circ. No. 5731
Freedman, W. L., *et al.* 1993, ApJ (submitted)
Garnavich, P., & Ann, H. B. 1993, IAU Circ. No. 5731; corrigendum: IAU Circ. No. 5733
Gomez, G., & Lopez, R. 1993, IAU Circ. No. 5733
Goodrich, R. W., Stringfellow, G. S., Penrod, G. D., & Filippenko, A. V. 1989, ApJ, 342, 908
Hamuy, M., & Suntzeff, N. B. 1990, AJ, 99, 1146
Hamuy, M., Suntzeff, N. B., Bravo, J., & Phillips, M. M. 1990, PASP, 102, 888
Hamuy, M., Suntzeff, N. B., Gonzalez, R., & Martin, G. 1988, AJ, 95, 63
Hill, R. S., *et al.* 1992, ApJ, 395, L37
Hobbs, L. M. 1969, ApJ, 157, 135
Hobbs, L. M. 1974, ApJ, 191, 381
Hobbs, L. M. 1976, ApJ, 203, 143
Hobbs, L. M. 1978, ApJ, 222, 491
Holm, A., & Crabb, W. 1979, IUE Newslett., 7, 40
Humphreys, R. M. 1993, private communication
Humphreys, R. M., Aaronson, M., Lebofsky, M., McAlary, C., & Strom, S. E. 1986, AJ, 91, 808
Humphreys, R. M., & Aldering, G. 1993, private communication
Humphreys, R. M., Jones, T. J., & Sitko, M. L. 1984, AJ, 89, 1155
Hutchings, J. B., Massey, P., & Bianchi, L. 1987, ApJ, 322, L79
Jannuzi, B., Schmidt, G., Elston, R., & Smith, P. 1993, IAU Circ. No. 5776
Jeffery, D. J. 1993, private communication
Kaufman, M., Bash, F. N., Kennicutt, Jr., R. C., & Hodge, P. W. 1987, ApJ, 319, 61
Landolt, A. U. 1992, AJ, 104, 340
Leibundgut, B., & Pinto, P. A. 1992, ApJ, 401, 49
Lewis, J., *et al.* 1993, MNRAS (submitted)
Martin, R., & Lewis, J. 1993, Gemini, 40, 14
Massey, P., Hutchings, J. B., & Bianchi, L. 1985, AJ, 90, 2239

Mattei, J. A. 1993, observations from the AAVSO international data base, private communication
Merlin, J.-C. 1993, IAU Circ. No. 5740
Moffat, A. F. J., & Vogt, N. 1977, PASP, 89, 323
Montgomery, K. A., Marschall, L. A., & Janes, K. A. 1993, AJ, 106, 181
Morrison, L. V., Argyle, R. W., & Helmer, L. 1993, IAU Circ. No. 5767
Nandy, K., Morgan, D. H., Willis, A. J., Wilson, R., Gondhalekar, P. M., & Houziaux, L. 1980, Nature, 283, 725
NASA 1993, in Inside Astrophysics, a NASA newsletter, v. 3, no. 2, p. 6
Neely, A. W. 1993a, IAU Circ. No. 5740
Neely, A. W. 1993b, IAU Circ. No. 5832
Nomoto, K. 1993, private communication
Nomoto, K., Filippenko, A. V., & Shigeyama, T. 1990, A&A, 240, L1
Nomoto, K., Suzuki, T., Shigeyama, T., Kumagai, S., Yamaoka, H., & Saio, H. 1993, Nature, 364, 507
Panagia, N. 1987, in High Energy Phenomena around Collapsed Stars, edited by F. Pacini (Reidel, Dordrecht), p. 33
Phillips, J. A., & Kulkarni, S. R. 1993, IAU Circ. No. 5763
Phillips, M. M., Wells, L. A., Suntzeff, N. B. Hamuy, M., Leibundgut, B., Kirshner, R. P., & Foltz, C. B. 1992, AJ, 103, 1632
Podsiadlowski, Ph., Hsu, J. J. L., Joss, P. C., & Ross, R. R. 1993, Nature, 364, 509
Pooley, G. G., & Green, D. A. 1993, IAU Circ. No. 5751
Porter, A. C. 1993, private communication
Ray, A., Singh, K. P., & Sutaria, F. K. 1993, A&A, 14, 53
Richmond, M. W., Treffers, R. R., & Filippenko, A. V. 1993, PASP (in press)
Ripero, J. 1993, IAU Circ. No. 5731
Sandage, A., & Tammann, G. A. 1974, ApJ, 194, 559
Sandage, A., & Tammann, G. A. 1987, A Revised Shapley-Ames Catalog of Bright Galaxies (Carnegie, Washington, D.C.)
Schild, R. E. 1983, PASP, 95, 1021
Schmidt, B. P., *et al.* 1993a, Nature, 364, 600
Schmidt, B. P., Eastman, R. G., & Kirshner, R. P. 1993b, in preparation
Sembach, K. R., Danks, A. C., & Savage, B. D. 1993, A&AS, 100, 107
Shelton, I. K. 1993, AJ, 105, 1895
Spitzer, L. Jr. 1978, Physical Processes in the Interstellar Medium (Wiley, New York), p. 156
Swartz, D. A., Clocchiatti, A., Benjamin, R., Lester, D. F., & Wheeler, J. C. 1993, Nature (in press)
Tanaka, Y. 1993, IAU Circ. No. 5753
Trammell, S. R., Hines, D. C., & Wheeler, J. C. 1993, IAU Circ. No. 5780
Tsvetkov, D. Yu. 1986, Sov. Astron. Lett., 12, 328
Van Dyk, S. D., Weiler, K. W., Rupen, M. P., Sramek, R. A., & Panagia, N. 1993, IAU Circ. No. 5759
Vidal-Madjar, A., Andreani, P., Ferlet, R., Cristiani, S., & Lanz, T. 1987, A&A, 177, L17
Wamsteker, W., Rodriguez, P. M., Gonzalez, R., Sonneborn, G., & Kirshner, R. 1993, IAU Circ. No. 5738
Weiler, K. W., Sramek, R. A., Van Dyk, S. D., & Panagia, N. 1993, IAU Circ. No. 5752
Wheeler, J. C., *et al.* 1993a, IAU Circ. No. 5737
Wheeler, J. C., *et al.* 1993b, ApJL (submitted)
Woosley, S. E., Eastman, R. G., Weaver, T. A., & Pinto, P. A. 1993, ApJ (submitted)
Woosley, S. E., Pinto, P. A., Martin, P. G., & Weaver, T. A. 1987, ApJ, 318, 664
Yun, M. S., Ho, P. T. P., & Lo, K. Y. 1992, ApJ, 411, L17
Zimmerman, H. U., *et al.* 1993, IAU Circ. No. 5748